UNIVERSITA' DEGLI STUDI DI PADOVA

Dipartimento di Istologia, Microbiologia e Biotecnologie Mediche

SCUOLA DI DOTTORATO DI RICERCA IN BIOCHIMICA E BIOTECNOLOGIE
INDIRIZZO BIOTECNOLOGIE

CICLO XXI

Involvement of TGF-β1 in Multimerin-2, but not Emilin-2 regulation of blood pressure

Direttore della Scuola : Ch.mo Prof. Giuseppe Zanotti

Supervisore :Ch.mo Prof. Giorgio M. Bressan

Dottorando : Dario Bizzotto

THESIS CONTENTS

NOMENCLATURE

The name of members of the EMILIN gene family undergoes several changes. After input from members of the EMILIN research community the nomenclature of the EMILIN family was reworked to clarify the relationships between the genes in this family. The nomeclature that has now been adopted is reported in table 1(http://www.genenames.org/genefamily/emilin.html). Human genes are indicated in capital letters (e.g. EMILIN1) whereas in murine genes only the first letter is written in capital (e.g. Emilin1). Moreover, genes are written in italics (e.g. *EMILIN1*) whereas protein names are written with normal character and a dash between name and number (e.g. EMILIN-1).

Human gene nomenclature (Chr location)	Aliases	Human gene sequence	Mouse ortholog (Chr location)	Mouse gene sequence
EMILIN1 (2p23.3-p23.2)	EMILIN, DKFZP586M121, EMILIN-1, gp115	NM_007046	*Emilin1* (5 B1)	NM_133918
EMILIN2 (18p11.3)	EMILIN-2, FLJ33200, FOAP-10	NM_032048	*Emilin2* (17 E1.3)	NM_145158 BC053753
MMRN1 (4q22)	ECM, EMILIN4,MMRN	NM_007351	*Mmrn1* (6 B3)	AK036724
MMRN2 (10q23.31)	Mmrn2, FLJ13465, ENDOGLYX-1, EndoGlyx-1, EMILIN3	NM_024756	*Mmrn2* (14 B)	NM_153127
EMILIN3 (20q12)	Emilin3, C20orf130, EMILIN5	XM_029741	*Emilin3* (2 H3)	NM_182840
EMID1 (22q12.2)	EMU1, hEmu1, Emu1, CO-5	NM_133455	*Emid1* (11 A1)	NM_080595
EMID2 (7q22.1)	EMU2, hEmu2, COL26A1	NM_133457	*Emid2* (5)	NM_024474

Table 1: Nomenclature for EDEN superfamily

ABBREVIATIONS

BMP: bone morphogenic protein
bp: base pair
BSA: bovine serum albumine
C-terminal: carboxyl terminal
DMEM: Dulbecco's modified Eagle medium
DTT:1,4-Dithiothreitol
E: embryonic age
ECM: extracellular matrix
ECs: endothelial cells
EDTA: ethylenediaminetetraacetic acid
EST: expressed sequence tag
FBS: foetal bovine serum
GAG: glycosaminoglycane
HRP: horseradish peroxidase
LAP: latency associated peptide
LLC: large latent complex
LTBP: latent TGFβ-binding protein
MCSA: media cross-sectional area
MFS: Marfan's Syndrome
Neo^R: neomicine resistance
NP40: Nonidet P40
N-terminal: amino terminal
ORF: open reading frame
PBS: phosphate-buffered saline
PECAM: Platelet endothelial cell adhesion molecule
PGK: phosphoglicerate kinase
PCR: polimerase chain reaction
SD: standard deviation
SEM: standard error of the mean
SLC: small latent complex
SMC: smooth muscle cells
TBS: Tris buffered saline
TGF-β: transforming growth factor beta
TK: timidine kinase

ABSTRACT

Emilins are a family of extracellular matrix (ECM) glycoproteins characterized by a cysteine-rich N-terminal EMI domain. The family comprises four members in mammals: Emilin-1, Emilin-2, Multimerin-1 and Multimerin-2. The prototype of this family is Emilin-1, a protein widely distributed in interstitial connective tissue in association with elastic fibers and strongly expressed in the mouse cardiovascular system during development and in the adult. *Emilin1* knockout animals display increased blood pressure, increased peripheral vascular resistance, and reduced size of arterial tunica media. The mechanism that brings about this phenotype entails an increase of TGF-β1 signalling with consequences on vascular SMC growth, ECM homeostasis, and vascular remodelling. It has been found that Emilin-1, through its EMI domain, binds proTGF-β1 and prevents its maturation by proprotein convertases. Therefore, Emilin-1 has an important role in the regulation of TGF-β extracellular availability.

To gain insight into the function of two other members of the Emilin family, *Emilin2* and *Mmrn2*, knockout mice for these genes were generated. Both genes are expressed mainly in the cardiovascular system: during development Emilin-2 was mainly found in the heart and blood vessels of the central nervous system, while in the adult it was detected in lymphoid organs and, with fainter staining, in heart and kidney. The expression of Multimerin-2 was restricted to endothelium.

The pattern of expression of these genes and the high sequence similarity with Emilin-1 (particularly in EMI domain) stimulated the analysis of the phenotype of the cardiovascular system in mutant mice.

Mmrn2 and *Emilin2* knockout mice were found to be hypertensive. For Multimerin-2 this alteration is accompanied by a mild reduction of the media cross-sectional area, whereas this is not the case for Emilin-2. Moreover, *Mmrn2* null mice exhibit an increased contraction of resistance vessels in response to the adrenergic α1 agonist phenylephrine. On the contrary, the response of *Emilin2*-/- blood vessels to this drug was normal.

Molecular mechanisms by witch Emilin-2 and Multimerin-2 carry out their physiological function in blood vessels were studied through *in vivo* and *in vitro* biochemical study. Evidences *in vitro* demonstrate that Emilin-2 and Multimerin-2 could reduce TGF-β1 signalling through the inhibition of proTGF-β1 processing into the LAP/TGF-β complex. This activity is mediated by

the EMI domain and the formation of a supramolecular association of Emilins with proTGF-β1 (or the LAP/TGF-β complex) was demonstrated.

The relevance of TGF-β1 in the pathogenesis of cardiovascular phenotype was tested by experiments *in vivo*, in which the *TGF-β1* gene dosage was genetically reduced in *Emilin2* and *Mmrn2* null mice. The hypertensive phenotype was rescued in *Mmrn2* knockout mice, while the blood pressure remained elevated in *Emilin2* null animals.

Different isoforms of TGF-β are expressed in the cardiovascular system during development and the inhibitory effect of Emilin-2 on TGF-β2 and -β3 signalling was demonstrated through *in vitro* assays. However, inactivation of a single *TGF-β2* allele did not reverse the hypertensive phenotype of *Emilin2*-/- mice, indicating that TGF-β2 dysregulation is not involved in the pathogenesis of this phenotype.

In conclusion the observations that Multimerin-2 produced by endothelial cells is able to regulate contractility of arterial vessels (due to vascular SMC) to adrenergic stimulation and that the hypertensive phenotype of null mice is caused by increased TGF-β1 signalling led to hypothesize that endothelial cells through expression of TGF-β1 regulate contractility of vascular SMC. Multimerin-2, localized between endothelial cells and vascular SMC, reduces the amount of TGF-β1 available to vascular SMC. Therefore, lack of Multimerin-2 gives rise to an increased signalling of TGF-β1 in vascular SMC that became more susceptible to sympathetic stimulation. Increased contractility of vascular SMC in small resistance vessels increases peripheral resistance and leads to hypertension. The cytostatic effect of TGF-β1 on vascular SMC and the consequent reduction in vessels size contribute to the generation of hypertensive phenotype.

The mechanism of regulation of blood pressure by Emilin-2 remains to be elucidated. The role of TGF-β3 in blood pressure homeostasis supposed from data *in vitro* needs to be verified *in vivo*. The involvement of other members of the TGF-β family of growth factors will also be considered in the future.

ABSTRACT (Italiano)

Le Emiline costituiscono una famiglia di glicoproteine della matrice extracellulare caratterizzate dalla presenza, all'estremità amino-terminale, di un dominio ricco di cisteine, denominato EMI. Nei mammiferi la famiglia comprende 4 membri: Emilina-1, Emilina-2, Multimerina-1, Multimerina-2. Emilina-1 è il prototipo per questa famiglia ed è largamente distribuita, in associazione con le fibre elastiche, nei tessuti connettivi interstiziali. Il sito di maggior espressione di Emilina-1 è il sistema cardiovascolare, sia durante lo sviluppo embrionale, sia nell'adulto.

Animali deficienti di Emilina-1 presentano una elevata pressione sanguigna associata ad un aumento delle resistenze vascolari periferiche ed una riduzione del diametro della tonaca media delle arterie. Il meccanismo che porta a questo fenotipo coinvolge un aumento di segnalazione di TGF-β1 con effetti riguardanti la crescita delle cellule muscolari lisce vascolari, l'omeostasi della matrice extracellulare e il rimodellamento vascolare. E' stato dimostrato che Emilina-1, mediante il dominio EMI, lega il proTGF-β1 e previene la sua maturazione da parte di proprotein convertasi. Emilina-1 ha quindi un importante ruolo nella regolazione della disponibilità del TGF-β nell'ambiente extracellulare.

Per comprendere la funzione di *Emilina2* e *Multimerina2* sono stati generati topi con un'inattivazione genica mirata di questi geni. Il sito di maggiore espressione di entrambi i geni è il sistema cardiovascolare. Durante lo sviluppo embrionale, Emilina-2 è principalmente presente nel cuore e nei vasi del sistema nervoso centrale mentre nell'adulto è stata trovata negli organi linfoidi e, in piccola quantità, nel cuore e nel rene. L'espressione di Multimerina-2 è invece ristretta agli endoteli.

La distribuzione di queste proteine e la loro elevata omologia di sequenza con Emilina-1 (in particolare a livello del dominio EMI) hanno guidato l'analisi del fenotipo dei topi mutanti verso il sistema cardiovascolare.

I topi deficienti di Emilina-2 e Multimerina-2 sono ipertesi. Per quanto riguarda Multimerina-2, il fenotipo ipertensivo è accompagnato da una leggera riduzione dell'area della tonaca media in sezione trasversale. Inoltre i topi deficienti di Multimerina-2 presentano un'aumentata contrattilità dei vasi di resistenza in risposta alla fenilefrina, un agonista dei recettori α_1 adrenergici. Nei topi deficienti di Emilina-2 invece questi due parametri risultano essere paragonabili ai topi di ceppo selvatico.

I meccanismi molecolari attraverso i quali Emilina-2 e Multimerina-2 svolgono le loro funzioni fisiologiche nei vasi sanguigni sono stati studiati attraverso studi *in vivo* e studi biochimici *in vitro*. Questi ultimi hanno dimostrato che Emilina-2 e Multimerina-2 possono ridurre la segnalazione di TGF-β1 attraverso l'inibizione della trasformazione del proTGF-β1 nel complesso LAP/TGF-β. Questa attività, mediata dal dominio EMI, si sviluppa attraverso la formazione di un'associazione sovramolecolare con il proTGF-β (o il complesso LAP/TGF-β).

L'importanza del TGF-β1 nella patogenesi del fenotipo cardiovascolare è stata testata attraverso esperimenti *in vivo*. Il dosaggio genico di *TGF-β1* è stato geneticamente ridotto nei topi deficienti di Emilina-2 e Multimerin-2. Il fenotipo ipertensivo è stato perso dai topi con inattivazione del gene *Multimerina2* mentre la pressione sanguigna rimane elevata nei topi in cui il gene *Emilina2* è stato inattivato.

Durante lo sviluppo embrionale, le diverse isoforme di TGF-β (TGF-β1, -β2 e -β3) sono espresse nel sistema cardiovascolare. Mediante saggi *in vitro* è stato dimostrato che Emilina-2 ha un effetto inibitorio anche sulla segnalazione di TGF-β2 e TGF-β3. Tuttavia, l'inattivazione di un allele di *TGF-β2* in topi deficienti di Emilina-2 non porta alla perdita del fenotipo, indicando che una deregolazione della segnalazione di TGF-β2 non è coinvolta nella patogenesi di questo fenotipo.

In conclusione, l'osservazione che Multimerina-2 prodotta dalle cellule endoteliali è in grado di regolare la contrazione delle arterie (dovuta alle cellule muscolari lisce vasali) in risposta alla stimolazione adrenergica e che il fenotipo ipertensivo è causato da un aumento della segnalazione di TGF-β1, porta ad ipotizzare che le cellule endoteliali, attraverso l'espressione di TGF-β1, possono regolare la contrattilità delle cellule muscolari lisce vasali. Multimerina-2, localizzata tra le cellule endoteliali e le cellule muscolari lisce, riduce la quantità di TGF-β1 disponibile per le cellule muscolari lisce. In conseguenza la mancanza di Multimerina-2 porta ad un aumento della segnalazione di TGF-β1 alle cellule muscolari lisce che diventano più sensibili alla stimolazione simpatica. Un aumento della contrattilità delle cellule muscolari lisce nei piccoli vasi di resistenza genera un aumento delle resistenze periferiche che portano quindi all'ipertensione. L'effetto citostatico del TGF-β1 sulle cellule muscolari lisce e la conseguente riduzione del calibro vasale contribuiscono alla generazione del fenotipo ipertensivo.

Il meccanismo di regolazione della pressione sanguigna da parte di Emilina-2 rimane inspiegato. I dati *in vitro* lasciano supporre un ruolo del TGF-β3 nella regolazione della pressione sanguigna

che deve però essere verificato *in vivo*. In futuro, inoltre, dovrà essere considerato anche il coinvolgimento di altri membri della famiglia dei TGF-β.

INTRODUCTION

EXTRACELLULAR MATRIX AND CELL SIGNALLING

The extracellular matrix (ECM) is a complex three-dimensional network of secreted macromolecules produced by different cell types. In addition to provide tissues with mechanical strength and stability, the ECM influences cell behaviour by the regulation of signals acting on the cell membrane. The best characterized of these functions is the adhesive one, that entails the assembly of signalling complexes at the cytoplasmic side of specialized sites of contact of the cells with the ECM called focal adhesions (Zamir and Geiger, 2001). The ECM can also affect cell behaviour in a way similar to growth factors, i.e. by binding surface receptors linked to specific signalling pathways (O'Reilly *et al.*, 1997). In addition, some ECM molecules modulate the activity of important growth factors like transforming growth factors beta (TGF-βs) and bone morphogenetic proteins (BMPs) (Zhu *et al.*, 1999; Bornstein, 2001). Moreover, growth factors can be stored as inactive complexes bound to the ECM and be released under particular conditions (Taipale and Keski-Oja, 1997) or specific components of the ECM may directly influence cell proliferation and differentiation (Karnik *et al.*, 2003). These functions of the ECM are particularly important in tissue morphogenesis during development and in pathological conditions, where they contribute to the refinement and/or the recovery of tissue structure (Taipale and Keski-Oja, 1997).

ELASTIC FIBERS

Elastic fibers are a component of the ECM responsible for elastic recoil and especially abundant in tissues such as lung, skin and, in particular, blood vessels. Biochemical and ultrastructural analysis have demonstrated that elastic fibers are constituted by two morphologically distinct component (Fahrenbach *et al.*, 1966; Greenlee *et al.*, 1966): a central amorphous nucleus consisting of Elastin and responsible for the elastic properties of the fiber; and microfibrillar elements, composed primarily by Fibrillin-1 and –2, highly organized and arranged as a coating of the amorphous core (Sakai *et al.*, 1986; Zhang *et al.*, 1994). The structural complexity and the functional properties of this component are not fully understood and are now emerging thanks to genetic analysis in the mouse. For instance, Fibrillin-1 is involved in most cases of Marfan

syndrome (MFS) (Collod-Beroud and Boileau, 2002). Marfan patients often exhibit emphysema; mice with mutations of the *Fibrillin1* gene also develop emphysema and it has been shown that this pathological alteration is due to dysregulation of TGF-β activation and signalling, resulting in apoptosis in the developing lung (Neptune et al., 2003). Another component of elastic fibers with regulatory activity is Elastin; null mice for this gene die soon after birth due to fibrocellular proliferation of the media layer that reduces considerably the lumen of blood vessels (Li *et al.*, 1998a). In fact, Elastin, a non-adhesive protein, inhibits cell proliferation via a non-integrin, heterotrimeric G-protein-coupled pathway and the observed alterations are due to lack of this inhibition (Karnik *et al.*, 2003). Interestingly, Elastin has also a role in determining the structure of blood vessels: heterozygous mutant mice have an increased number of elastic lamellae (Li *et al.*, 1998b), and loss of function of one *ELASTIN* allele in humans induces sopravalvular aortic stenosis, in which narrowing of the vessel's wall is the consequence of the increased thickness of the media determined by a higher number of elastic lamellae (Curran *et al.*, 1993). Although the molecular details of how these modifications are brought about are not known, they indicate that Elastin has important effects on the behaviour of vascular cells. Interestingly, *Elastin* null heterozygous mice develop arterial systemic hypertension (Faury et al., 2003). This trait is also observed in mice deficient of *Fibulin5* (Yanagisawa et al., 2002) and *Emilin1* (Zacchigna *et al.*, 2006), two other components of elastic fibers. All these data strongly suggest that elastic fibers are key modulators of vascular cells function and that, through action on the cells, they regulate structural remodelling of blood vessels and important physiological parameters such as arterial blood pressure.

Emilin-1

Emilin-1, initially named gp115, was isolated from chicken aorta and found to be particularly abundant in that tissue (Bressan *et al.*, 1983). Immunofluorescence studies confirmed that this protein is strongly expressed in blood vessels and revealed its presence in the connective tissue of a wide variety of organs (Colombatti *et al.*, 1985). At the ultrastructural level, the molecule was detected in elastic fibers, where it was located at the interface between the amorphous core and the coat of microfibrils (the name Emilin is an acronym assembled from Elastin Microfibrils Interface Located proteIN) (Bressan *et al.*, 1993). Emilin-1 appears in early stage of aorta development in association with a network of maturing microfibrils. Moreover, the process of elastic fibers formation was altered by anti-Emilin antibodies suggesting that the protein may be

involved in elastogenesis (Bressan *et al.*, 1993). The role of the protein in elastic fibers assembly was confirmed with the disruption of the *Emilin1* gene in mice. *Emilin1* null mice have a normal development and are morphologically indistinguishable from wild-type littermates, but a closer examination shows alteration in elastic lamellae of elastic arteries and cellular defects in morphology and anchorage (Zanetti *et al.*, 2004). Emilin-1 presents a multimodular structure including a C-terminal gC1q domain similar to those of type VIII and type X collagens endowed with cell adhesion-promoting functions (Colombatti *et al.*, 2000); a short uninterrupted collagenous stalk and a long α-helical domain with high probability for coiled-coil structure formation in the central part; a unique cysteine-rich sequence of approximately 80 amino acids, the EMI domain, that follows the signal peptide and forms the N-teminal end of the mature molecule (Colombatti *et al.*, 2000). Studies on Emilin-1 have demonstrated that the gC1q domain is necessary for the formation of non-covalent homotrimers and acts as a nucleation centre for triple helix and multimers formation (Mongiat *et al.*, 2000). Moreover, it was demonstrated that Emilin-1, through its C1q domain, promotes adhesion of smooth muscle cells (Doliana *et al.*, 1999) by the interaction with integrin $\alpha_4\beta_1$ (Spessotto *et al.*, 2003).

Studies on *Emilin1* null mice have revealed two striking phenotypes. One concerns the cardiovascular system, in which the protein is expressed both during development (Braghetta *et al.*, 2004) and in the adult. *Emilin1* deficient mice exhibit a generalized reduction of arterial diameter, increased peripheral resistance and systemic arterial hypertension (Zacchigna *et al.*, 2006). More recent studies have shown that Emilin-1 is involved in the regulation of the growth and in the maintenance of the integrity of lymphatic vessels. Indeed, *Emilin1* deficiency results into hyperplasia and enlargement of lymphatic vessels and in a reduction of anchoring filaments (Danussi *et al.*, 2008). The lymphatic vessels of *Emilin1* null mice are functionally altered, leading to a mild lymphedema associated with inefficient lymph drainage and increased leakage.

THE EDEN (EMILIN/MULTIMERIN) SUPERFAMILY

It was later realized that *Emilin1* is member of a larger group genes, identified as the EDEN (EMI Domain ENdowed) (or Emilin/Multimerin) superfamily, distinguished by the presence of the N-terminal EMI-domain (Doliana *et al.*, 2000; Braghetta *et al.*, 2004). The presence of cysteine-rich domains has been reported in various proteins, including several constituents of elastic fibers or protein associated with them. For instance, Fibrillin-1 contains at least five different types of cysteine-rich motifs (Sinha *et al.*, 1998). The EMI domain, however, is rather

unique since it is characterized by seven cysteine residues while most of the cysteine-rich domains described to date contain either six or eight. Moreover, the distribution of cysteines in EMI domain is conserved: distances between C1 and C2, C5 and C6, and C6 and C7 are absolutely conserved, whereas minimal gaps are present between C2, C3 and C4 (Doliana *et al.*, 2000). In mammals the EDEN superfamily comprises seven members: *Emilin1, Emilin2, Multimerin1, Multimerin2, Emilin3, Emid1* and *Emid2* (figure 1). The first four genes share extensive homology and represent the Emilin family proper within the superfamily (Colombatti *et al.*, 2000; Braghetta *et al.*, 2004). High sequence similarity between Emilins was found in EMI and gC1q domains. In particular, bioinformatics analysis of human and murine EMI domains revealed an average similarity of 60%. Moreover, the seven cysteines of EMI domains are located at highly conserved positions: although the total lengths of domains are variable between 71 to 79 aminoacids, the distances between cysteines are conserved. Only the second cysteine is shifted downstream of four residues in Multimerin-2, while it is absent in Multimerin-1 (Doliana *et al.*, 2000EMI a novel). Emilin-3 is the sole member of the truncated Emilin family and is characterized by the lack of the C-terminal gC1q domain. Emids are part of a separate family, being formed by the EMI domain followed by a collagenous domain with some triple helix interruptions (Leimeister *et al.*, 2002).

This thesis will deal principally with two members of the Emilin protein family, *Emilin2* and *Multimerin2*. For this reason, information on these two molecules is given below.

Emilin-2

Human *EMILIN2* was identified in a yeast two-hybrid screen using the globular gC1q domain as bait (Doliana *et al.*, 2001), while the sequence of the murine counterpart was deduced from the cDNA isolated form a differential screen of cochlear cDNA (Amma *et al.*, 2003). The human protein contains 8 potential N-glycosilation site and 20 cysteines that could be involved in intracellular disulfide bond. Analysis of the entire primary sequence demonstrated that this protein is highly homologous to EMILIN-1. This high homology may have a functional correlate, as EMILIN-2 and EMILIN-1 may form mixed oligomers via their C-terminal gC1q domain and the potential coiled coil domain (Doliana *et al.*, 2000). The EMI domain at the N-terminus is much more conserved between these two proteins in comparison to the other EMI domain-containing gene products. The short collagenic stretch of 17 triplets GXY in EMILIN-1 is conserved in EMILIN-2, although in the latter there are four variations. One striking

difference between the two proteins was that in EMILIN-2 an unusually 55-residue-long proline-rich domain, in which the proline content exceeds 41%, precedes the collagenic region. This domain might be implicated in additional protein-protein interactions (Doliana *et al.*, 2000). The close identity between *EMILIN1* and *EMILIN2* cDNAs is further emphasized by their gene organization, which is almost identical (Doliana *et al.*, 2001). In situ hybridization, RT-PCR have revealed a specific and, in part, overlapping expression profile of Emilin-2 with respect to Emilin-1 (Braghetta *et al.*, 2004). During development Emilin-2 was found in extraembryonic tissues such as visceral endoderm and in ectoplacental cone, but, at variance with Emilin-1, this expression was rapidly lost at later embryonic stage. Strong expression was found in maternal tissues: hybridization signal was present in decidual cells, particularly at the hilar side. In the embryo, Emilin-2 was present in different tissues but strongest expression was found in the heart, starting at E8.5 and reaching highest levels at E11.5. Unlike other member of the Emilin family, staining for Emilin-2 was found in the central nervous system. Expression levels of Emilin-2, like Emilin-1 and Multimerin-2, decrease during postnatal development with a pattern dependent on the organ. In adult, Emilin-2 was mainly expressed in heart, but it was also present in spleen and uterus while weaker expression was found in kidney and gut (Braghetta *et al.*, 2004).

The biological function of Emilin-2 is unclear: a recent study *in vitro* suggests that EMILIN-2 is able to induce apoptosis through a death receptor-mediated mechanism. EMILIN-2 promotes cell death by the activation of the extrinsic apoptotic pathway through direct interaction with the TRAIL receptors DR4 and DR5. Therefore this ECM protein could be considered as a modulator of cell survival (Mongiat *et al.*, 2007).

Multimerin-2

Multimerin-2, initially named Emilin3, was initially identified *in silico* through comparison of human and murine ESTs present in GenBank (Doliana *et al.*, 2000). In human, MULTIMERIN-2 coincides with EndoGlyx-1, a cell surface glycoprotein complex with an apparent molecular mass of approximately 500 kDa. This complex is composed of four different disulfide-bonded protein species (p110, p125, p140 and p200): p125 and p140 derive from a common mRNA and differ for the amount of glycosylation, while the derivation of the additional subunits p110 and p200 was not characterized. (Christian *et al.*, 2001). Immunohistochemistry analysis revealed that the expression of this protein is restricted to endothelium of blood vessels, while it is not

present in non-endothelial cells and in endothelial cells of hepatic and splenic sinusoids. This restricted distribution suggested a potential role of this protein in vasculogenesis, angiogenesis and hemostasis (Christian *et al.*, 2001). EndoGlyx-1 immunostaining was found also in tumour capillaries, including "hot spots" of neoangiogenesis in certain tumours (Sanz-Moncasi *et al.*, 1994).

The cDNA of murine *Mmrn2* codifies for a 943 residues long protein containing the N-terminal EMI domain and the C-terminal gC1q domain, characteristic of the Emilin family genes. Between the central coiled-coil region and gC1q domain, Multimerin-2 presents a peculiar cluster of basic aminoacids with a consensus for the binding with GAG (like heparin and heparan-sulfate) found in proteins that bind heparin like von Willebrand factor (unpublished data, P. Bonaldo).

In mice, *Mmrn2* mRNA was detected in morulae, blastocysts and undifferentiated ES cells by RT-PCR. In situ hibridization revealed the presence of *Mmrn2* in extraembrionic and maternal tissue with an expression pattern complementary to *Emilin2*. *Emilin2* mRNA was detectable in extraembryonic visceral endoderm while *Mmrn2* labeling was found in chorionic plate. In addition, *Emilin2* was faintly expressed in ectoplacental cone while weak staining for *Mmrn2* was found in allantois. In embryo *Mmrn2* expression was restricted to endothelium with a maximum of expression between E9.5 and E11.5 (Braghetta *et al.*, 2004).

TRANSFORMING GROWTH FACTOR βs

TGF-β1 is the prototypic member of a large family of evolutionarily conserved pleiotropic secreted cytokines, which also includes Activins and BMPs. Individual family members have crucial roles in multiple processes throughout development and in the maintenance of tissue homeostasis in adult life (Massague and Gomis, 2006; Feng and Derynck, 2005). Not surprisingly, therefore, subversion of signalling by TGF-β family members has been implicated in many human diseases, including cancer, fibrosis, autoimmune and vascular diseases (Blobe *et al.*, 2000). TGF-β family members signal via two related single transmembrane spanning type I and type II receptors endowed with serine/threonine kinase activity (Heldin *et al.*, 1997; Schmierer and Hill, 2007). Each ligand has a specific set of type II and type I receptors with which it interacts. In particular, in most cases, TGF-β interacts with TGF-β RII and TGF-β RI also termed activin receptor-like kinase 5 (ALK5) (Franzén *et al.*, 1993). In endothelial cells

TGF-β can also signal via activin receptor-like kinase 1 (ALK1) (Goumans *et al.*, 2002). The type I receptors act downstream of type II receptors and determine the signalling specificity within the receptor complex. Upon ligand-induced heteromeric complex formation, the type II receptor constitutively active kinase domain trans-phosphorylates the type I receptor (Wrana *et al.*, 1994). The activated type I receptor propagates the signal into the cell by phosphorylating specific receptor-regulated (R-) Smads at two C-terminal serine residues (Souchelnytskyi *et al.*, 1997). TGF-β and activins in most cases signal via R-Smad2 and Smad3 that, when activated, form heteromeric complexes with common mediator (Co-) Smad, (i.e., Smad4 in mammals), which accumulate in the nucleus. There they can bind to DNA promoter elements and act as transcription factor complexes together with other transcription factors, co-activators and co-repressors (Massague and Gomis, 2006; Feng and Derynck, 2005).

Despite the large number and distinct functions of TGF-β family members (33 in mammals), there is an enormous convergence in signalling to only five type II receptors, seven type I receptors and two main Smad intracellular pathways. The high number of ligands is best explained by the need for finely tuned developmental patterns of receptor activation, which is achieved in part by differential regulation of ligand expression and activation from latent complexes. (Massague and Gomis, 2006; Feng and Derynck, 2005)

Signalling specificity and diversity could be generated by different mechanisms. A single ligand often activates several type II-type I receptor combinations. Since the signalling responses are defined by the composition of the receptor complex, in particular that of the type I receptor, a ligand can induce different responses, depending on the nature of the activated receptor complexes. For example, in endothelial cells, TGF-β can activate two distinct type I receptor/Smad signalling pathways with opposite effects. Whereas the TGF-β/ALK5 pathway leads to inhibition of cell migration and proliferation, the TGF-β/ALK1 pathway induces endothelial cell migration and proliferation (Goumans *et al.*, 2002). Moreover, inhibitory Smads (Smad6 and Smad7) inhibit TGF-β family signalling primarily by competitively interfering with R-Smad for type I receptors binding (Imamura *et al.*, 1997; Nakao *et al.*, 1997). Smads cooperate through physical interactions with remarkable diversity of DNA sequence-binding transcription factors. The regulation of the activities of the interacting transcription factors by other signalling pathways further defines this cooperation. In addiction to interactions with DNA-binding transcription factors, Smads can recruit coactivators or corepressors into the transcription machinery that determine the amplitude of TGF-beta/Smad-mediated transcriptional activation (Feng and Derynck, 2005).

Extracellular regulation of TGF-β signalling by co-receptors (which control the access of ligands to signalling receptors) and interplay between TGF-β ligands and extracellular molecules that regulate the activity of these ligands could be important mechanisms that control signalling specificity (ten Dijke and Arthur, 2007).

The access of TGF-β ligands to their receptors is controlled by two classes of molecules with opposing function. One class includes membrane-anchored proteins that act as accessory receptors, or coreceptors, promoting ligand binding to the signalling receptors. The membrane-anchored proteoglycan betaglycan, also known as the TGF-β type III receptor, has long been known to mediate TGF-β binding to the type II receptor, a role that is particularly critical for TGF-β2 (Brown *et al.*, 1999). Endoglin is required for efficient TGF-β signalling through TGF-β RII-ALK1 in endothelial cells (Lebrin *et al.*, 2004). The other class of molecules comprises a diverse group of soluble proteins that act as ligand binding traps, sequestering the ligand and barring its access to membrane receptors. They include the small proteoglycan decorin and the circulating protein α2-macroglobulin, which bind to free TGF-β; follistatin, which binds to Activins and BMPs; and three distinct protein families-Noggin, Chordin/SOG, and DAN/Cerberus-whose members also bind to BMPs (Shi and Massaguè, 2003). This class also include the proregion of TGF-β precursor; all three TGF-β isoforms (TGF-β1, TGF-β2 and TGF-β3 in mammals) are secreted in latent forms that need to be activated before they can bind to signalling receptors (Annes *et al.*, 2004). TGF-βs are synthesized as precursor proteins that are proteolytically processed. The signal peptide is removed from the pre-pro-TGF-β during transit through the rough endoplasmic reticulum and, following dimerization, another cleavage occurs by the convertase family of endoproteases (Dubois *et al.*, 1995). These proteases cleave the precursor into the C-terminal mature peptide and the N-terminal precursor remnant (also known as latency associated peptide (LAP)) within the secretory vesicles or in the extracellular space (Beck *et al.*, 2002; Zacchigna *et al.*, 2006). Control and/or localization of convertase activity may represent an important level of regulation of TGF-β ligands. After cleavage, mature TGF-β and LAP remain associated via non-covalent bonds to form the LAP/TGF-β complex also called small latent complex (SLC). LAP shields the receptor interacting surface of TGF-β and this keeps the growth factor in its latent form (Annes *et al.*, 2004; ten Dijke and Arthur, 2007). The SLC can covalently bind to the latent TGFβ-binding protein (LTBP) to form the large latent complex (LLC) (Saharinen *et al.*, 1996).

After secretion, the LLC binds to the ECM via the N-terminal domain of LTBP and localization of LTBP to the ECM is required for effective TGF-β activation (Nunes *et al.*, 1997). LTPBs stabilize latent TGF-β complexes and regulate their activation at the cell surface (Rifkin, 2005). Moreover, LTBPs might target the latent TGF-β complex to specific sites, including structural components within the elastic fibres, where they may be stored for later use.

Functional analysis through gene ablation in mice is an important part of understanding how these signal transduction pathways functions *in vivo*; these studies have demonstrated the importance of TGF-β signalling in development and disease (Goumans and Mummery, 2000). The importance of TGF-β pathway in vascular morphogenesis was revealed by the targeted inactivation of TGF-β signalling components in mice, which die at midgestation during embryogenesis due to disrupted vasculogenesis in the yolk sac (ten Dijke and Arthur, 2007).

Targeted disruption of *TGF-β* genes in mice results in various alterations that are summarized in table 2.

Model	Phenotype	Refs
TGF-β1	Defective yolk sac vasculogenesis and haematopoiesis. Embryonic lethal (E9.5-11.5). Inflammation and autoimmunity	Dickson *et al.*, 1995; Shull *et al.*, 1992; Kulkarni *et al.*, 1993; Letterio *et al.*, 1996
TGF-β2	Cardiac, lung, craniofacial, limb, spinal column, eye, inner ear, urogenital defects. Perinathal lethality.	Sanford *et al.*, 1997
TGF-β3	Cleft palate, delayed lung maturation. Mutants die shortly after birth.	Proetzel *et al.*, 1995; Kaartinen *et al.*, 1995

Table 2: Major defect in *TGF-β* deficient mice.

In mice, targeted disruption of the *TGF-β1* gene results in diffuse and lethal inflammation: *TGF-β1* null mice at approximately 3 weeks of age develop a progressive wasting syndrome, resulting in death within a few days (Shull *et al.*, 1992; Kulkarni *et al.*, 1993). However, an embryonic phenotype has been described in *TGF-β1* null mice as only 50% of the conceptuses reach parturition (Shull *et al.*, 1992; Kulkarni *et al.*, 1993; Dickson *et al.*, 1995). Investigating the prenatal lethality, Dickson and co-workers showed that 50% of the *TGF-β1*−/− and 25% of

TGF-β1+/− mice died by embryonic day E10.5 due to defective haematopoiesis and endothelial differentiation of extraembryonic tissue,

TGF-β2 ablated mice display a wide range of developmental defects and perinatal lethality (Sanford *et al.*, 1997). Malformations include cardiac, lung, craniofacial, limb, spinal column, eye, inner ear and urogenital defects. *TGF-β2*−/− mice exhibit a subset of the following structural heart defects: (a) small descending aorta with a thin or hypoplastic wall; (b) aortic and pulmonary orifices both leading to the right ventricle, both showing patent valve leaflets; and (c) tricuspid and mitral valves both connected to the left ventricle. Therefore, it can be speculated that TGF-β2 plays a role in normal and possibly abnormal cardiac morphogenesis (Bartram *et al.*, 2001).

Targeted disruption of the *TGF-β3* gene results in defective palatogenesis and delayed pulmonary development. (Proetzel *et al.*, 1995; Kaartinen *et al.*, 1995).

TGF-β REGULATION BY ELASTIC FIBER COMPONENTS

Recent studies recognized that ECM proteins play a crucial role in the regulation of cytokine bioavailability in the vascular system, in particular, the release of latent TGF-β (ten Dijke and Arthur, 2007). Elastic fibers, the component responsible for elastic recoil of tissues like blood vessels lung and skin, are a good example of the role of extracellular matrix in cell signalling in addition to the mechanical one. Support to this concept comes from recent data on gene knockout experiments of elastic fiber constituents

The SLC can covalently attach to the large latent TGFβ-binding protein (LTBP) to form the large latent complex (LLC) (Saharinen *et al.*, 1996). LTBPs are required for the secretion and correct folding of TGF-βs (Miyazono *et al.*, 1991). The association with LTBPs results in the storage of latent TGF-β in ECM structures rapidly after secretion.

Four different LTPBs have been identified, of which LTBP1, LTBP3 and, to a lesser degree, LTBP4 covalently bind to LAPs of all three TGF-β isoforms (Saharinen and Kei-Oja, 2000). Localization of LTBP to the ECM is required for effective TGF-β activation (Nunes et al., 1997): LTPBs stabilize latent TGF-β complexes and regulate their activation at the cell surface (Rifkin, 2005). The significance of this interaction *in vivo* was examined by inactivation of these genes in mice. The *Ltbp1* disruption induces a reduced biological activity of TGF-β (Drews *et al.*, 2008). The pathological changes of the *Ltbp-3* null mice are consistent with perturbed TGF-

beta signalling (Dabovic *et al.*, 2002) and also the profound defects in the elastic fiber structure of *Ltbp-4* knockout mice are associated with reduced deposition of TGF-beta in the extracellular space (Sterner-Kock *et al.*, 2002).

Recent *in vitro* evidences revealed that lysyl oxidase (LOX), an amine oxidase critical for the initiation of collagen and elastin cross-linking and founded in elastic fibers suppressed TGF-β1 signalling likely through its amine oxidase activity and binding of mature TGF-β1 (Atsawasuwan *et al.*, 2008).

Another component of elastic fibers with regulatory activity is Fibrillin1, the gene involved in most cases of Marfan syndrome (Collod-Beroud and Boileau, 2002).

MFS syndrome is a systemic disorder of connective tissue. Cardinal manifestations include proximal aortic aneurysm, dislocation of the ocular lens, and long-bone overgrowth (Judge and Dietz, 2005). Moreover, distinct subgroup of individuals with MFS present emphysema, which frequently results in spontaneous lung rupture (Wood *et al.*, 1984).

It was initially thought that aortic aneurysms in MFS were due to structural defects in the aorta resulting from a failure to stabilize elastic-fibre structure when fibrillin1 was limiting. The resultant elastin fragmentation in the aortic wall would make the aorta susceptible to injury from haemodynamic forces. Recently, it has become clear that an important function of fibrillin1 is to control TGF-β bioavailability. Mice deficient in *Fbn1* develop MFS phenotypic manifestations (Neptune *et al.*, 2003; Carta *et al.*, 2006). Reduced fibrillin1 may result in incorrect LLC sequestration and excessive activation of TGF-β signalling, a major contributory factor in the vascular pathology of MFS (Neptune *et al.*, 2003; Habashi *et al.*, 2006). In lung of *Fbn1*-/- mice, abnormalities are evident in the immediate postnatal period and manifest as a developmental impaiment of distal alveolar septation. In the developing lung, dysregulation of TGF-β activation and signalling results in apoptosis (Neptune *et al.*, 2003).

All these data suggest a crucial role of ECM proteins in regulation of TGF-β bioavailability in the vascular system. Defects in ECM, which were initially thought to affect the physical properties of vessels wall and thereby compromise the vasculature, are now linked to enhanced TGF-β-Smad signalling.

EMILIN1 LINKS TGF-β MATURATION TO BLOOD PRESSURE HOMEOSTASIS

Emilin1 null mice have a hypertensive phenotype caused by increased peripheral resistance. Hyperthension in these mice is likely caused by developmental perturbation on vessel size. A relevant cause of *Emilin1* phenotype is the reduced vSMC growth due to excess of TGF-β signalling (Zacchigna *et al.*, 2006). Using *Xenopus laevis* embryos and mammalian cell-culture techniques, Zacchigna and co-workers established a role for Emilin-1 as a negative regulator of TGF-β signalling. In particular, Emilin-1, through its EMI domain, inhibits TGF-β1 signalling by binding specifically to the immature proTGF-β1 precursor and preventing its maturation by furin proprotein convertases. Together, the biochemical and functional evidences have revealed an intriguing role for Emilin-1 that acts as one of the earliest extracellular regulators of TGF-β1 signalling. This activity is relevant in the context of blood vessels; in fact, the inactivation of a single *TGF-β1* allele in *Emilin1* null mice was sufficient to bring blood pressure levels back to normal (Zacchigna *et al.*, 2006).

Evidences associating TGF-β with hypertension has steadily been accruing: serum TGF-β level was correlated to blood pressure (Suthanthiran *et al.*, 2000) and an association between polymorphisms in the *TGF-β* gene and hypertension has also been reported (Cambien *et al.*, 1996). Experimental evidence suggests, for Emilin-1, a pathogenetic mechanism in which lack of this protein in vascular cells increases proteolytic processing of proTGF-β1. This results into increased activation of TGF-β1 and enhanced signalling, whose major effect is inhibition of vascular smooth muscle cells proliferation. As a consequence, the size of vessels of the arterial tree is decreased and the lower diameter of resistance vessels increases peripheral resistance of blood vessels with ensuing hypertension (Zacchigna *et al.*, 2006).

AIM OF THE RESEARCH

Large part of information about the Emilin gene family concerns Emilin-1. In particular, function *in vivo* was studied only in *Emilin1* null mice. The phenotype of these mice involves lymphatic vessels and the cardiovascular system, where the phenotype was linked to an increased TGF-β1 signalling. Evidences about other Emilins regard mainly gene and protein structure and expression. This thesis expands the investigation of the function to two other

members of the Emilin family, *Emilin2* and *Multimerin2*, with the use of knockout mice for these genes generated in my laboratory. The aim of this work is the comprehension of molecular mechanisms by which Emilin-2 and Multimerin-2 carries out its physiological function. The analysis was restricted to cardiovascular system in which both *Emilin2* and *Multimerin2* null mice present a hypertensive phenotype.

EXPERIMENTAL PROCEDURES

MOUSE STRAINS AND PROCEDURES

Procedures involving animals and their care were conducted according to institutional guidelines in compliance with national laws. *Emilin1–/–* mice were generated as previously described (Bonaldo et al., 1998; Zanetti *et al.*, 2004) using standard procedures (Nagy *et al.*, 2003). Isolation of homologous recombinant embryonic stem cells clones and microinjection of the cells into blastocysts were carried out by Prof. P. Bonaldo and Dr. P. Braghetta (Department of Histology, Microbiology and Medical Biotechnologies, University of Padova, Padova, Italy). Mice carrying a null mutation in the *TGF-β1* gene were kindly provided by A.B. Roberts (National Cancer Institute, National Institutes of Health, Bethesda, MD, USA). Mice carrying a *TGF-β2* null allele were purchased from Jackson Laboratories (Ann Arbor, Maine, USA). All animals used in experiments here described were 2-4 months of age.

IMMUNOHISTOCHEMISTRY

Mouse tissues and E13.5 embryos were embedded in OCT (Sakura), snap-frozen, and stored at -80°C. Cryostatic sections (7 μm) were collected on positively charged slides (BDH Superfrost Plus), air dried at room temperature and kept at -80°C. Before being used, the sections were equilibrated at room temperature and hydrated with phosphate-buffered saline (PBS) for 5 min. Immunostaining against Emilin2 was performed after antigen unmasking with ialuronidase (Sigma, 0.5U/μl in NaCl 50 mM, $NaCH_3COOH$ 20 mM, pH 6.0) for 1 hour. Then, the sections were saturated with the blocking buffer (10% goat serum in PBS) for 30 min. Primary and secondary antibodies were diluted in 5% goat serum. The antibodies used were the following: polyclonal rabbit anti-Emilin-2 (gift from Prof. D. Forrest); monoclonal rat anti-PECAM (Santa Cruz Biotechnology, Inc.); monoclonal rat anti-Multimerin-2 (gift from Prof. A. Colombatti); goat anti-rat IgG Cy3-conjugated antibody (Jackson Immuno Research); goat anti-rabbit IgG Cy2-conjugated antibody (Jackson Immuno Research); goat anti-rat IgG Cy-2 conjugated antibody (Jackson Immuno Research). Slides were incubated for 2 h at room temperature or overnight at 4°C with the primary antibody. For immunofluorescence, secondary antibody was applied for 1 h at room temperature. Nuclei were visualized with propidium iodide (Sigma). The

slides were mounted in 80% glycerol in PBS and observed in a Zeiss Axioplan microscope equipped with epifluorescence optics or in a Bio-Rad confocal microscope. For immunoperoxidase, endogenous peroxidase activity was blocked with 3% hydrogen peroxide in PBS for 30 minutes before primary antibody incubation. The slides were developed with a biotin-labeled secondary antibody (Vectastain ABC kit produced by Vector Laboratories, Inc.). Then, the AB Complex/HRP was added and sections were stained with 3,3'-diaminobenzidine substrate (0.5 mg/ml in 50 mM Tris-HCl pH 7.5) (Sigma).

NORTHERN BLOTTING AND REVERSE TRANSCRIPTASE PCR (RT-PCR) ANALYSIS

RNA was extracted from normal and mutant embryos or tissues by using TRIzol reagent (Gibco-BRL) as recommended by the manufacturer. For Northern blot analysis, 15 μg of total RNA were separated in 1% agarose–formaldehyde gels, blotted onto Hybond-N membranes (Amersham), and hybridized at 42.8°C with ^{32}P-labeled probes synthesized from cDNA clones using standard procedures (Ausubel et al., 1993). Filters were washed in 0.1x SSC/ 0.1% SDS at 68°C. The probe used is a 1.8-kb fragment spanning the exon 5 of murine Emilin-2 cDNA (gift from A. Colombatti).

RT-PCR analysis was performed as follows. First strand cDNA synthesis using 1 μg total RNA and random hexanucleotides was performed with M-MLV reverse transcriptase (Invitrogen). Amplification was carried out in 50 μl reaction mixtures containing 0.1–0.3 μg cDNA, 10 mM Tris–HCl pH 9.0, 50 mM KCl, 1.5 mM MgCl2, 0.1% Triton X-100, 0.2 mM dNTPs, 25 pmol of each primer and 2U Taq DNA polymerase (Fynnzymes). The reaction products were separated in 1-2 % agarose gels and stained with ethidium bromide. The oligonucleotides used for these reactions are reported in Table 3. To correct for sample variations in RT-PCR efficiency, the amplification of Eif1a (Eukaryotic translation initiation factor 1a) was used as internal control.

CELL CULTURE AND TRANSFECTION

HEK293T cells were cultivated in Dulbecco's Modified Eagle's Medium (DMEM) containing 4.5g/L glucose, 25 mM Hepes, 2mM L-Glutamine (Invitrogen) and supplemented with 10% fetal

bovine serum (Invitrogen), 100 U/ml penicillin and 100 µg/ml streptomycin (Invitrogen). Cells were maintained at 37°C in a humidified 5% CO_2 atmosphere.

Primer	Sequence
1	5'-GGG TTC AAG CCG TGT ACT A-3'
2	5'-ACC ACC CCA TGA GTT ATT GC-3'
3	5'-GGG AAA GAG CCA AAG GGT TA-3'
4	5'-GTC ACG TTT CGG AGA GGG AAG T-3'
5	5'-TGT GGG GCT CAA GAT GTG T-3'
6	5'-GGG GTC TCC TGA CAC ATC TTG A-3'
7	5'-GCC CAG TGC CAG GAA CAA AAA CT-3'
8	5'-AAC TCT CGC TTC CCT CCT GT-3'
9	5'-GGA CAA CGT TTT CTT AGG CTG AG-3'
10	5'-TGC TGA ATG GAC GGC TGG ACA A-3'
11	5'-TCT GCG TTC TTC TCC GTC AC-3'
12	5'-CCA GAC AGC TGT GGA AGT GA-3'
13	5'-TGG AAC AAC AGC CCA TGT TA-3'
14	5'-GCC AGA GGC CAC TTG TGT AG-3'
15	5'-CGC TAT CAG GAC ATA GCG TTG G-3'
16	5'-TCG CCT TCT TGA CGA GTT CT-3'
17	5'-CGG ATC CCT CAG AAG AAC TCG T-3'
18	5'-CAT CTG GTT CCA GGG ACA GT-3'
19	5'-TGC CAA GAA GGT CCC AAA GAC-3'
20	5'-ACT GGA GAT CCA GCA CCA TC-3'
21	5'-GTG GGC AGC TTG TGG AAC TG-3'
22	5'-TGG TCC TGC AGG GTC TTC TG-3'
23	5'-CAA GTA GCG CCC GTC GTA TG-3'
Mmrn2-for	5'-CTC ACC CTG ATC CCG ACA CT –3'
Mmrn2-rev	5'-GTC TGA TGG GGT CTC TGC TG-3'
Eif1a-for	5'-AAG AAG TCT GAA GGC CTA TG-3'
Eif1a-rev	5'-CAG AGA ACT TGG AAT GTA GC-3'

Table 3: Oligonucleotides used in RT-PCR analysis of Emilin-2 transcripts.

Cells were plated at 50% confluence on 60 mm diameter plates an transfected with the indicated plasmids using the calcium phosphate method (Sambrook *et al.*, 1989). Briefly, DNA dissolved in 250 mM $CaCl_2$ was added dropwise to an equal volume of 2x Hepes-buffered saline (HBS) (280 mM NaCl; 10 mM KCl; 1.5 mM Na_2HPO_4; 12 mM dextrose; 50 mM Hepes) with gentle mixing. Calcium phosphate-DNA coprecititates solution was added dropwise to the Petri dish and immediately mixed by swirling. After 6-8 hours the culture medium was changed and incubation continued for 12-20 hours. Before harvesting, cells were cultivated in serum-free medium (OPTIMEM-Glutamax I, Invitrogen) for 36-48 hours.

DNA CONSTRUCTS

Cloning of mouse *Emilin1*, *Emilin1* EMI domain and *Emilin1*ΔEMI in pCS2+ expression vector were previously described in Zacchigna *et al.*, 2006. Mouse *Emilin2* cDNA was retrotranscribed from E13.5 total RNA, PCR amplified and cloned into XhoI-XbaI sites (underlined) of pCS2+ vector. The following oligonucleotides were used: 5'-AAC TCG AGT GTG GGG CTC AAG ATG TGT-3' (forward) and 5'-AAT CTA GAT TCT TCC CTT CCT GGT CTC-3'. Mouse *Emilin2* EMI domain (aminoacids 1-222) was generated by PCR using *Emilin2* full length cDNA as template and cloned into XhoI-XbaI site (underlined) of pCS2+. The forward primer was the same used for full length *Emilin2* cloning, whereas the reverse primer was 5'-AAT CTA GAC TAA TCA TCT TGA ATG GTG TGT TT-3'. *Emilin2*ΔEMI contains the deletion of aminoacids 48-223. cDNA coding for aminoacids 1-47 were generated by PCR with the forward primer used for full length *Emilin2* cloning and the reverse primer 5'-AAG GCG CCG TTC CTG GCA CTG GGC CT-3' containing a NarI site (underlined). The 3' sequence coding for aminoacids 224-1074 was generated with the following oligonucleotides: 5'- AAG GCG CCG GCA GAA AAG AGC CAG ACT-3' (forward, containing a NarI site) and reverse primer used for full length cDNA cloning. These two fragments were joined by NarI restriction and ligated into the XhoI and XbaI sites of pCS2+. *Emilin2* EMI domain-GPI -FLAG codes for a GPI membrane-anchored version of the EMI-domain fused at the N-terminus to the Chordin signal peptide and the FLAG epitope (Larrain *et al.*, 2000). cDNA coding for *Emilin2* EMI domain (aminoacids 36-222) was generated by PCR using full length *Emilin2* as template and the following oligonucleotides: 5'-AAC TCG AGC AGC CTG GGT ACC ACG CG-3' (forward) and 5'-AAA CCG GTA TCA TCT TGA ATG GTG TGT TTG-3' (reverse, containing AgeI site, underlined). GPI anchoring sequence was prepared using plasmid EMI-domain-GPI in

Zacchigna *et al.*, 2006 as template and the following primer: 5'-AAA CCG GTT TTT CAG ACC TAT GGA AAC TAA C-3' (forward, containing AgeI site, underlined) and 5'-AAT CTA GAT TAT GTC AGA AGC CCC ATA GTA-3' (reverse containing XbaI site, underlined). These two fragments were joined with AgeI restriction and inserted in XhoI-XbaI sites of pCS2-Chd-FLAG (gift from S. Piccolo), in which cDNA was cloned in frame with the signal peptide of Chordin and the FLAG epitope. Mouse *Mmrn2* full length cDNA was retrotranscribed from total mouse lung RNA and cloned into ClaI-XbaI site (underlined) of pCS2+ vector. The following oligonucleotides were used: 5'-AAA TCG ATC TCA CCA TGA TCC CGA CAC T-3' (forward) and 5'-AAT CTA GAC AGG CGG ATC TAC CAT GTC T-3' (reverse). Mouse *Mmrn2* EMI domain (aminoacids 1-232) was generated by PCR using *Mmrn2* full length as template and cloned into BamHI-XbaI site (underlined) of pCS2+. Forward primer was 5'-AAG GAT CCC TCA CCA TGA TCC CGA CAC T-3' whereas reverse primer was 5'-AAT CTA GAC TAA TGG GGC TGC AGC AGG TG-3'. *Mmrn2*ΔEMI has been deleted of aminoacids 55-232. cDNA coding for aminoacids 1-54 were generated by PCR with forward primer used for *Mmrn2* EMI domain and reverse primer 5'-AAC TCG AGT CTG ATG GGG TCT CTG CTG-3' containing a XhoI site (underlined). 3' sequence coding for aminoacids 233-943 were generated with the following oligonucleotides: 5'-AAC TCG AGA TTG ATG CAT TCC TGA AAG CAC-3' (forward, containing XhoI site, underlined) and reverse primer used for full length *Mmrn2* cDNA cloning. These two fragments were joined by XhoI restriction and ligated in BamHI and XbaI site of pCS2+. *Mmrn2* EMI domain GPI anchor FLAG tagged was generated as follow: cDNA coding for *Mmrn2* EMI domain (aminoacids 23-232) was generated by PCR using full length *Mmrn2* as template and the following oligonucleotides: 5'-AAC TCG AGC AGG ACC CCG GTA CCA AGT-3' (forward) and 5'-AAA CCG GTA TGG GGC TGC AGC AGG TGC T-3' (reverse, containing AgeI site, underlined). The fragment coding for GPI anchoring sequence was prepared as described for *Emilin2* EMI domain GPI anchored FLAG tagged. Two fragments were joined with AgeI restriction and inserted into XhoI-XbaI sites of pCS2-Chd-FLAG. Mouse *Elastin* full length cDNA was cloned in pCS2+ by Dr. M. Milanetto. FLAG-tagged TGF-β1 is described in Zacchigna *et al.*, 2006. Mouse constitutively active proTGF-$\beta 2^{C226S/C228S/C229S}$ and mouse constitutively active proTGF-$\beta 3^{C228S/C230S}$ were generated by site-directed mutagenesis by overlap extension (Higuchi *et al.*, 1988) of cysteine residues essential for latency that are located in conserved positions of LAP. Briefly, one pair of primers was used to amplify the DNA that contains the mutation site together with upstream sequences. The second pair of primers was used to amplify the DNA that contains the mutation site together

with downstream sequences. The two sets of primers were used in two separate amplification reactions to amplify overlapping DNA fragments. The mutations of interest were located in the region of overlap. The overlapping fragments were mixed, denaturated, and annealed to generate heteroduplexes that can be extended and amplified into a larger DNA fragment using two primers that bind to the extremities of the two original fragments. Cysteines 226, 228 and 229 of mouse proTGF-β2 were mutated in serines as follows. Mouse pro*TGF-β2* cloned in pCMV-SPORT6 (RZPD) was used as template. A fragment of pro*TGF-β2* spanning from Eco47III site and BamHI site of cDNA was mutated. The first pair of oligonucleotides was: 5'-CCA AAG ACT TAA CAT CTC CCA CC-3' (forward) and 5'-CGA AGG TAC **T**GC **T**GG GGC **T**GT-3' (reverse with mutations, bold letters). The second pair was: 5'-AC**A** GCC CC**A** GC**A** GTA CCT TCG-3' (forward with mutations, bold letters) and 5'-ATG CCC CAG CAC AGA AGT TAG C-3' (reverse). The mutated DNA was cloned in pGEM-T easy vector (Promega) and sequenced. This mutated part of TGF-β2 was subcloned into pCMV-SPORT6-TGF-β2 by BamHI and Eco47III restriction. Restriction with SpeI excised mutated TGF-β2 that was then subcloned into pCS2+ XbaI site to produce proTGF-$\beta2^{C226S/C228S/C229S}$. Cysteines 228 and 230 of TGF-β3 were mutated as follows. Mouse pro*TGF-β3* cloned into pCMV-SPORT6 (RZPD) was used as template. In order to produce mutated fragment of pro*TGF-β3* comprised between the two BglII sites of cDNA sequence, three fragments were generated by PCR. The following primers amplified 5'-end of this fragment (spanning from 5'-BglII and Eco47III siteof cDNA): 5'-CGT TGG ACT TCG GCC ACA TC-3' (forward) and 5'-CCT ATG TAG CGC TGC TTG GC-3' (reverse). Mutation of central fragment (spanning from Eco47III to NheI sites of cDNA) were generated by two primers pairs: first pair: 5'-CAG CTC CAA GCG CAC AGA AC-3' (forward) and 5'-GTG TGA C**T**T GGA C**T**G TGG ATG-3' (reverse with mutations, bond letters). Second pair: 5'-CAT CCA C**A**G TCC A**A**G TCA CAC-3' (forward with mutations, bond letters) and 5'-CCA CCT CTG CCT GCA CCA C-3' (reverse). The 3'-end of the fragment (spanning from NheI and 3'-BglII site of cDNA) was amplified with 5'-GAG GCC TGG AGC CCA GAA G-3' (forward) and 5'-CCA GGG GAC TTT GGC TTG GT-3' (reverse) primers. Fragments were inserted into pGEM-T easy vector (Promega) and sequenced. The 5' fragment was cut with SphI (present in pGEM-T easy vector) and Eco47III and inserted into the same restriction site of mutated fragment in pGEM-T easy (SphI site of vector and Eco47III site of the inserted fragment) to form 5' mutated fragment in pGEM-T easy. 3' fragment isolated by NheI site and SalI (site present in the vector) digestion was subcloned into the same restriction site of 5'-

mutated fragment to produce the whole mutated fragment of proTGF-β3$^{C228S/C230S}$ in pGEM-T easy. This construct was digested with BglII and the fragment was subcloned in BglII restricted mouse proTGF-β3$^{C228S/C230S}$ in pCMV-SPORT6. The full length proTGF-β3$^{C228S/C230S}$ was isolated by BamHI and NarI digestion and subcloned into pCS2+.

All PCRs were performed by Expand High Fidelity PCR System (Roche). Recombinant plasmids were propagated in *E. coli* DH5α, and plasmid DNA was isolated and purified in milligram batches by column chromatography using PureYield^{TM} Plasmid Maxiprep System (Promega), according to the manufacturer's recommendations.

LUCIFERASE ASSAY

HEK293T cells were transfected using the calcium phosphate method (as described above) with the following plasmids: CAGA12-LUX reporter for TGF-β activity (gift from P. ten Dijke); porcine constitutively active proTGF-β1$^{C223S/C225S}$ (gift from J.M. Davidson) or mouse constitutively active proTGF-β2$^{C226S/C228S/C229S}$ or mouse constitutive active proTGF-β3$^{C228S/C230S}$; pCMV-LacZ (gift from S. Piccolo) for normalization for transfection efficiency; expression plasmids coding for tested proteins. Cell layers were harvested with luciferase lysis buffer (25 mM Tris-HCl pH 7.8; 2.5 mM EDTA; 10% Glycerol; 1% NP40; 2 mM DTT) after 24 hours of starvation in DMEM supplemented with 0,1% FBS. Luciferase and β–galactosidase activity were measured in each sample and values of luciferase activity were normalized on β-galactosidase activity to account for differences of transfection efficiencies. Every sample was transfected in triplicate, and every experiment was repeated at least two times

WESTERN BLOTTING

Aortas dissected from 8 weeks old *Multimerin2*+/+, +/– and –/– mice were cleaned from surrounding tissue and adventitia, frozen in liquid nitrogen, pulverized by a mortar and powder was resuspended in lysis buffer (50 mM Hepes; 200 mM NaCl; 5 mM EDTA; 5% Glycerol; 1% NP40; 1x protease inhibitor cocktail (Roche); 1x Phosphatase inhibitor cocktail (Sigma)). Protein content was determined by the BCA method (Pierce). Samples from transfected HEK293T cells were collected in ice-cold NP40 lysis buffer (25 mM Tris-HCl pH 7.5; 2.5 mM EDTA; 1% NP40; 1x protease inhibitor cocktail). Sample loading was normalized for

differences of transfection efficiency on the basis of β-galactosidase activity (see above), and protein samples were resolved under reducing conditions by SDS-PAGE in 4-12 or 10% NuPAGE® Bis-Tris gels (Invitrogen) and blotted onto polyvinylidene difluoride membranes (Millipore). The filters were blocked with 5% non-fat dry milk (Biorad) in TBS 1x (TBS 10x: 80 g Tris; 24.2 g NaCl in 1 liter)-0.1% Tween20 (TBS-T) buffer and then incubated with the primary antibodies. Following washes with TBS-T buffer, the membranes were incubated with horseradish peroxidase-linked secondary antibodies (Amersham Bioscience) and reacting bands revealed with SupersignalWest-pico and -dura HRP substrates (Pierce). Primary antibodies used were: monoclonal rat anti-Multimerin-2 (gift from A. Colombatti), 1:15 dilution of hybridoma medium; M2 rabbit anti-Flag monoclonal antibody (Sigma), 1:1000 dilution; goat anti-LAP antibody (R&D systems), 1:1000 dilution; monoclonal mouse anti-β-actin (Sigma), 1:4000 dilution; polyclonal rabbit anti-Emilin-1 and anti-Emilin-2 (gift of D. Forrest), 1:1000 dilution.

IMMUNOPRECIPITATION

HEK293T cells were transfected with the indicated plasmids. After 48 hours of starvation in serum-free medium (see above), cells were harvested in ice-cold lysis buffer (25 mM Tris pH 7.5, 150 mM NaCl, 2.5mM EDTA, 10% Glycerol, 1%NP40, protease inhibitors cocktail (Roche)). Immunoprecipitation was performed using ExactaCruz™ C kit (Santa Cruz Biotechnology, Inc.) according to the manufacturer's recommendations. Briefly, 50 μl of IP matrix were mixed with 2 μg of goat anti-LAP antibody to form the IP matrix-antibody complex. After 4 hours of incubation at 4°C on a rotator, matrix was washed with PBS and incubated at 4°C on a rotator overnight with 80 μl of cell lysate diluted to 500 μl with dilution buffer (25 mM Tris-HCl pH 7.5; 150 mM NaCl; 1.5 mM $MgCl_2$; 1mM EDTA; 10% Glycerol; 0,1% BSA; protease inhibitors cocktail). After incubation, matrix was washed 3 times with wash buffer (50 mM Hepes pH 7.8; 150 mM NaCl; 5% Glycerol;0.5 mM; $MgCl_2$; 0.1% NP40) and then resuspended in 2x reducing final sample buffer (Invitrogen). Samples were boiled for 5 minutes and immunoblotted. Western blot primary antibody was detected with HRP conjugated ExactaCruz™ reagent via standard incubation and detection protocols.

EVALUATION OF BLOOD PRESSURE, VASCULAR REACTIVITY AND MEDIA CROSS-SECTIONAL AREA

Measurements of cardiovascular parameters in mice were carried out in the laboratory of Prof. G. Lembo (Department of Angiocardioneurology, I.R.C.C.S. Neuromed Institute, Pozzilli (IS), Italy). Here are briefly reported the experimental procedures used for these analysis.

Blood pressure was evaluated non-invasively by tail-cuff plethysmography.

Vascular reactivity in mesenteric arteries was tested as previously described (Lembo *et al.*, 2000). The main branch of the mesenteric artery was dissected out from each mouse and placed in cold Krebs-Henseleit bicarbonate buffer solution with the following composition (mmol/l): NaCl 118.3, KCl 4.7, $CaCl_2$ 2.5, $MgSO_4 \cdot 7H_2O$ 1.2, KH_2PO_4 1.2, $NaHCO_3$ 25, glucose 5.6. The mesenteric artery was cleaned of the adhering perivascular tissue and cut into rings 3 mm long. Mesenteric rings were suspended in isolated tissue baths filled with 20 ml Krebs solution continuously bubbled with a mixture of 5% CO_2 and 95% O_2 (pH 7.37-7.42) at 37°C. One end of the mesenteric rings was connected to a tissue holder and the other end to an isometric force transducer. The signal was passed to a Gould pressure processor and then acquired in a computerized system by Gould's Data Acquisition and Signal Analysis (DASA; Gould Instruments). The analysis of the generated curves was performed by the View II software (Gould Instruments) and the sensitivity of the system was 5 ± 1 mg of tension generated. The rings were equilibrated for 90 min in the unstretched condition, and the buffer was replaced every 20 min. The length of the smooth muscle was increased stepwise in the equilibration period to adjust passive wall tension to 0.5 g. Once basal tension was established, the length of the rings was not altered thereafter. Caution was taken to avoid endothelium damage. Contraction to phenylephrine (10^{-9} - 10^{-6} mol/l) was tested.

Evaluation of media cross-sectional area was made as follow: mesenteric vessels corresponding to the second branch (~140 to 200 μm of average diameter in relaxed conditions) were excised free of connective and adipose tissue and two stainless steel wires of 40 μm of diameter were threaded through the lumen. This ring preparation was mounted on a micromyograph, as previously described (Vecchione *et al.*, 2002). Vessels were then equilibrated and relaxed for at least 30 minutes in Krebs solution kept constantly at 37°C and bubbled with 5% CO_2 in O_2. After equilibration, the micromyograph was transferred to the stage of a light microscope with immersion lens connected to a charge-coupled device camera. The vessel was stretched slightly (wall tension about 0.1 N/m), and structural characteristics of the vessel were evaluated.

SEQUENCING AND BIOINFORMATIC SEQUENCE ANALYSIS

RT-PCR products were cloned into pGEM-T Easy (Promega) according to the manufacturer's protocol. Sequencing was performed with the Sanger method by BMR Genomics (Padova-Italy) with SP6 and T7 promoter primers.

Sequence alignments were performed with Basic Local Alignment Search Tool (BLAST) of National Center for Biotechnology Information (NCBI) website (http://www.ncbi.nlm.nih.gov). Prediction of splice site was carried out by Neural Network Splice Site Prediction Tool (NNSPLICE0.9) of Berkeley Drosophila Genome Project website (http://www.fruitfly.org/seq_tools/splice.html).

STATISTICAL ANALYSIS

For systolic blood pressure and MCSA, data were expressed as mean±SEM and a two-way ANOVA for repeated measures was used. A *P* value <0.05 was assigned statistical significance. For luciferase assay, data are expressed as mean± SD. The statistical significance of the results was determined by using Bonferroni test or Student's t-test. A *P* value <0.01 was considered significant.

RESULTS

DISTRIBUTION OF Emilin-2 AND Multimerin-2

Analysis of gene expression is relevant in the interpretation of gene targeting experiments. Previous studies on *Emilin2* and *Mmrn2* using *in situ* hybridization revealed that the genes are intensely expressed in the cardiovascular system. In particular, *Emilin2* appeared to be mainly expressed in the heart, starting at E8.5 and reaching highest levels at E11.5. Expression was restricted to the myocardium, while the endocardium was negative. Conversely, *Mmrn2* mRNA was detected only in endothelial cells and endocardium, with the highest levels between E9.5 and E11.5 (Braghetta *et al.*, 2004).

To better define the gene expression pattern, the distribution of Emilin-2 and Multimerin-2 were analyzed by immunoperoxidase and indirect immunofluorescence in embryos and adult organs. Immunoperoxidase of E13.5 embryos confirmed that Emilin-2 is mainly expressed in the heart (figure 2A). Immunofluorescence in sections of embryonic heart revealed that the protein is deposited in the extracellular matrix around muscle fibers of myocardium (figure 2C). Double immunofluorescence for Emilin-2 and the specific endothelial marker PECAM (*Platelet endothelial cell adhesion molecule*) showed no overlapping of staining, indicating that Emilin-2 is not synthesized by endothelial cells and by endocardium (figure 2D).

Emilin-2 was also localized in tail mesenchyme, where the protein has a metameric distribution corresponding to intervertebral disks anlage (figure 2A). Finally the protein was present in the mesenchymal tissue of anterior cranial region, genital tubercle, tongue (figure 2A) and in the blood vessels wall of the central nervous system (figure 2B).

The distribution of Emilin-2 was also examined in adult organs. Immunoperoxidase staining was present in lymphoid organs such as spleen, thymus and lymphnodes. In the spleen, Emilin-2 formed a thin network surrounding the central arteriole of the white pulp, where T lymphocytes form periarterial lymphatic sheaths, while the red pulp was negative (figure 3A). Emilin-2 was deposed in large vessels of medullar region of thymus, while smaller vessels that branch from it and are present in the cortical region are weakly stained (figure 3B). Emilin-2 was present in lymphnodes (figure 3C), principally in medullar cords (figure 3D). Adult heart expressed Emilin-2 that was deposed between the muscle fibers (figure 3E). Finally Emilin-2 was found in the medullar region of kidney as thin fibers between tubules (figure 3F).

Immunofluorescence for Multimerin-2 confirmed the association of the protein with the endothelium of blood vessels. aorta (figure 4A). Figures 4A and 4B show staining in aorta and mesenteric arteries respectively: the protein is located in the extracellular matrix between the internal elastic lamina and the basal side of endothelial cells.

CHARACTERIZATION OF *Emilin2* AND *Mmrn2* KNOCKOUT MICE

Emilin2 and *Mmrn2* knockout mice were generated in my laboratory through homologous recombination in ES cells as previously described (Bonaldo *et al*., 1998).

In the targeting construct for *Emilin2*, the neomycin resistance gene (neo^R), controlled by the 3-phosphoglicerate kinase (PGK) promoter in the same orientation of the *Emilin2* gene, replaced exon 2 and part of the second intron. Neo^R was flanked by two homology arms of 3.1 kb at the 5'- and 4 kb at 3'-end. The timidine kinase cassette (TK gene and promoter) for negative selection was placed at the 5'-end of the targeting construct (figure 5A).

In the *Mmrn2* targeting vector, the PGK-neo^R cassette in the reverse orientation replaced the first exon and was flanked by 4 kb and 7 kb of homology at the 5'- at 3'-end respectively. The TK cassette was placed at the 5'-end (figure 5B).

For *Emilin2*, two positive recombinant clones were identified and checked for correct single integration by Southern blot analysis. The clones were used to generate germ line chimeric mice by injection into C57BL/6 host blastocysts. The resulting male chimeras were bred to C57BL/6 females, to obtain heterozygous F1 mice, which were intercrossed to produce homozygous null mice. For *Mmrn2*, germline transmission of the mutation was obtained from four correctly targeted clones (Prof. P. Bonaldo and Dr. P. Braghetta).

In gene targeting methods, the correct insertion of the construct is not sufficient to assure a complete inactivation of gene expression. Aberrant splicing events could reconstitute mRNA coding for proteins with residual biological activity. This possibility must be avoided by analysis of the gene products.

In GenBank two entries for *Emilin2* cDNA were present. The first (accession number NM_145158) was isolated from a cochlear library from mice at postnatal day 8 (Amma *et al.*, 2003). This was a 3910 bp cDNA containing a complete 3224 bp open reading frame (ORF). The second (accession number BC053753), derived from a pool of undifferentiated limb mesenchyme and early condensing mesenchyme from mouse embryo of E10.5-E11.5 (Strausberg *et al.*, 2002), was 4283 bp long and contained the same 3224 bp ORF. mRNA from

E13.5 whole *Emilin2* wild-type and knockout embryos was analyzed through northern blotting (figure 6A). Wild-type mice showed a band of 4.5 kb that exceeded the size deduced from the GenBank sequences. This band had a decreased intensity in heterozygous mice and disappeared in null embryos that, instead, showed two bands of 5.6 and 4.2 kb. Therefore, a detailed analysis of mRNA from wild-type and null mice was needed to explain the presence of two bands in the knockout sample. Moreover, in order to avoid the possibility of an incomplete or aberrant knockout, it was necessary to exclude the presence of residual transcripts coding for truncated or modified forms of the protein because these may modify the mutant phenotype (Müller, 1999).
Alignment between the two *Emilin2* cDNA sequences and *M. musculus* chromosome 17 genomic sequence (Genbank accession number NT_039649) revealed the following data:

- Base 1 to 248 in NM_145158 sequence, has an additional 5'-UTR sequence in BC053753 entry. In this sequence, this exon spans from base 18 to base 532.
- The first 18 bases in BC053753 are part of an additional exon located upstream of exon 1 of NM_145158 entry. Therefore exons of Emilin2 gene rise from 8 to 9.

A detailed RT-PCR analysis was carried out in order to check the structure of both wild-type and mutant transcripts. Primers were designed in order to determine the structure of both wild-type and mutant transcripts. Primers location in the genomic sequence is shown in figure 6B. The results of RT-PCR analysis are summarized in Table 4.

- Primers 1-3 (figure 6C): sense and antisense oligonucleotides are located respectively in exon 1 and exon 2. The predicted band in wild-type cDNA was 160 bp long, whereas no band was expected in the null cDNA in which exon 2 was deleted. Wild-type sample presented a band of 350 bp corresponding to a transcript without splicing between exon 1 and exon 2. This is confirmed through amplification of genomic DNA that showed the same band (figure 6C, DNA lane). Contamination of RNA with genomic DNA was excluded by amplification of RNA sample without retrotranscription (figure 6C, RNA lanes).
- Primers 1-14 (figure 6D): primer 14 is complementary to neo^R cassette. A band of 125 bp was expected for the knockout allele, whereas no bands were expected wild-type sample because the neo^R cassette was not present. A band of 340 bp, corresponding to mRNA without splicing between exon 1 and neo^R cassette, was found in knockout sample. Amplification of RNA is negative and confirmed the absence of contamination with genomic DNA.

Primers	Figure	Predicted band (bp)	Result (bp)	Comments
1-3	6C	WT: 160 KO: -	WT: 350 KO: -	No splicing between exon 1 and exon 2 Exon2 deleted in KO mice
1-14	6D	WT: - KO: 125	WT: - KO: 340	Wild type mice have not neo^R cassette No splicing between exon1and neo^R cassette
1-2	6E	WT: 177 KO: 177	WT: 177 KO: 177	Lacking of splicing between exon1and exon 2 confirmed
1-8	6F	WT: 586 KO: 2233	WT: 230 KO: 230	Possibility of splicing between donor site in intron1and exon 3. In KO mice it result in deletion of neo^R cassette.
4-6	6G	WT: 199 KO: -	WT: 199 KO: -	Exon 2 deleted in KO mice
15-17	6H	WT: - KO: 155	WT: - KO: 155	Neo^R cassette inserted in null mice
7-9	6I	WT: 360 KO: -	WT: 360 KO: -	Proper splicing between exons 2-3, 3-4 and 3-5 in WT mice. Exon 2 deleted in KO mice
16-18	6J	WT: - KO: 976	WT: - KO: 140	Splicing *between* neo^R cassette and exon 3 in KO mice.
16-20	6K	WT: - KO: 1346	WT: - KO: 510	Wild type mice have not neo^R cassette. Splicing between neo^R cassette and exon 3 in KO mice
12-13	6L	WT: 285 KO: 285	WT: 285 KO: 285	Transcription proceed until 3'-UTR in both WT and null mice
10-11	6M	WT: 121 KO: 121	WT: 121 KO: 121	Both WT and KO alleles present exon 5
21-23	6N	WT: 726 KO: 726	WT: 726 KO: 726	Proper splicing between exons 5-6, 6-7, 7-8 and 8-9
19-22	6O	WT: 2124 KO: 2124	WT: 210 KO: 210	Possibility of splicing between exon4 and exon 6
Eif1a	6P	WT: 170 KO: 170	WT: 170 KO: 170	Normalization with housekeeping gene *Eukaryotic Translation Initiation Factor 1a*

Table 4: Summary of results of *Emilin2* transcripts analysis on wild type and *Emilin2* null mice by RT-PCR.
WT = wild type; KO = knockout

- Primers 1-2 (figure 6E): antisense primer is located in the first intron. The presence of the expected band in wild-type and null cDNA confirmed the lack of splicing between exon1 and, respectively, exon 2 or neo^R cassette.
- Primers 1-8 (figure 6F): primer 8 is placed in exon 3. The expected bands were 586 bp in wild-type and 2233 in null cDNA. In both samples RT-PCR amplified a band of 230 bp. This PCR product was unexplainable on the basis of the deduced exon structure of the gene (figure 6B). Sequencing of this fragment (figure 7A) demonstrated the presence of a splicing donor site in the first intron of the *Emilin2* gene. Therefore, an alternative splicing removes exon 2 in wild-type mice and neo^R cassette in knockout mice.
- Primers 4-6 (figure 6G): primers are complementary to exon 2. Lack of amplification in null cDNA confirmed the deletion of the exon.
- Primers 15-17 (figure 6H): primers are located in neo^R cassette. The amplification of the expected band in knockout cDNA confirmed the presence of the neo^R cassette.
- Primers 7-9 (figure 6I): sense primer is complementary to the junction of exon 2 and exon 3 in wild-type cDNA. Antisense primer is located in exon 5. Null allele lacks exon 2, therefore no band was expected. Proper splicing between exons 2-3, 3-4 and 4-5 in wild-type cDNA was confirmed by the amplification of the correct band.
- Primers 16-18 (figure 6J): primer 16 is placed in neo^R cassette, whereas primer 18 is in exon 3. The predicted PCR product is 976 bp long and comprises the 3' region of the neo^R cassette, part of the second intron and the 5' sequence of exon 3. Instead the mutant allele presented a band of 140 bp. Prediction of splice site with bioinformatics tools revealed the presence of a splice donor site located after the coding region of neo^R cassette. The length of PCR product matched with a mRNA deriving from a splicing between the donor site in neo^R cassette and acceptor site of exon 3.
- Primer 16-20 (figure 6K): antisense primer is placed in exon 5. The amplification of a 510 bp long product confirmed the splicing between neo^R cassette and exon 3 and correct splicing between exons 3-4 and 4-5.
- Primers 12-13 (figure 6L): these primers are located in the 3'- UTR region. The expected band was amplified from in both alleles, indicating the presence of exon 9 sequences in both transcripts
- Primer 10-11 (figure 6M): both primers are placed in exon 5. The presence of exon 5 in wild-type and mutant allele was confirmed by the amplification of the correct PCR product in both samples.

- Primer 21-23 (figure 6N): sense primer is complementary to exon 5, whereas the antisense oligonucleotide is located in exon 9. The expected band was present in both alleles. This data confirmed the proper splicing between exons 5-6, 6-7, 7-8 and 8-9.
- Primer 19-22 (figure 6O): primers are located in exon 4 and exon 6. The predicted band was 2124 bp long, but both samples presented a band of 210 bp. This length corresponds to a cDNA in which exon 5 is spliced out. The predicted fragment was not amplified. This is believable because amplification of longer fragment are disadvantage compared to smaller fragment.
- *Eukaryotic Translation Initiation Factor 1a* (figure 6P): the amplification of transcript for this housekeeping gene was used as loading control.

The above RT-PCR analysis allows to propose the structure of *Emilin2* transcripts shown in figure 7B. In wild-type embryos, splicing between exon 1 and exon 2 does not take place, resulting a mRNA species of 4.5 kb (figure 7B, transcript I).

In null mice the presence of two transcripts was confirmed (figure 7B): the first (5.6 kb) (figure 7B: transcript IV) begins before the neo^R cassette in exon 1 and continues along the *Emilin2* gene with a splicing between a donor site placed within the neoR cassette after coding region of neomycin resistance gene and the acceptor site of exon3. This mRNA should correctly code for neomycin transferase: in fact there is not site for beginning of translation before neo^R cassette and protein synthesis should stop at the end of the neomycin transferase ORF. The second transcript (4.2 kb) (figure 7B transcript V) results from a splicing between a donor site in intron 1 and the acceptor site of exon 3 that removes the neo^R cassette and presents a predicted ORF of 2978 bp. However, this putative ORF has not a ribosome-binding site, does not comply with reading frame of *Emilin2* and lacks a signal peptide necessary for the extracellular localization. A similar splicing seems to be possible in wild-type mice (figure 6F), giving rise to transcript II of figure 7B) that is not found is northern blot analysis (figure 6A). Probably this gene product is a minor species. Another alternative splicing was found between exon 4 and exon 6 in both wild-type and knockout transcripts (figure 7B: transcripts III and VI). mRNAs resulting from this splicing events were not found in northern blot analysis. In wild-type this transcript (figure 7B, transcript III) was 2.6 kb long and has a predicted ORF of 1311 bp coding for a putative protein of 436 aminoacids. In knockout mice, like transcript IV, transcript VI, that is 3.7 kb long, should also correctly code for neomycin transferase.

The absence of Emilin-2 in null mice was confirmed by immunoperoxidase with specific antibody in sections from embryos and adult tissues: Emilin-2 staining was present in wild-type

sections (figure 8A, C, E, G), while there was no staining in the knockout embryo (figure 8B, D, F, H).

Abolishment of Multimerin-2 expression in homozygous mutants was confirmed through study of both mRNA and protein. RT-PCR analysis with primers amplifying exon 1 showed that *Mmrn2* mRNA was absent in null mice (figure 9A). Deficiency of the protein was confirmed by immunofluorescence in sections of aorta from wild-type and knockout mice (figure 9B). Western blot analysis on aorta extracts validated this data: heterozygous mice displayed lower amount of Multimerin-2 than wild-type mice, while in knockout animals expression of the protein was completely suppressed (figure 9C).

Litters generated by *Emilin2* or *Mmrn2*+/– intercrosses exhibited a Mendelian distribution of genotypes (Table 5). Hetero- and homozygous mutant animals were fertile, had growth rates indistinguishable from that of controls, and did not show any gross abnormality. This finding suggests either compensatory effects from other Emilins or the presence of more subtle phenotypes in Emilin2 and Multimerin2 knockout mice.

A	+/+	+/-	-/-
Emilin2	161	297	132
%	27.3	50.3	22.4

B	+/+	+/-	-/-
Mmrn2	84	176	62
%	26.1	54.7	19.3

Table 5: Frequency of different *Emilin2* and *Mmrn2* genotypes in animals derived from crossing between heterozygote mice.

ANALYSIS OF THE VASCULAR PHENOTYPE OF *Emilin2* AND *Mmrn2* NULL MICE

Emilin-2 and Multimerin-2 are strongly expressed in the mouse cardiovascular system during development (Braghetta et al., 2004) and in the adult (this thesis). Moreover, the proteins present a high sequence similarity with Emilin-1, whose deficiency leads to a hypertensive phenotype in the mouse (Zacchigna et al., 2006). This observation prompted us to investigate cardiovascular structure and function of *Emilin2* and *Mmrn2* null animals. Measurements of cardiovascular parameters in mice were carried out in the Prof. G. Lembo laboratory (Department of Angiocardioneurology, I.R.C.C.S. Neuromed Institute, Pozzilli (IS), Italy). Systemic blood pressure measured by non-invasive methods was significantly increased in *Emilin2* and *Mmrn2* null mice compared to wild-type littermates, reaching levels similar to those of *Emilin1* null mice (figure 10A).

Increase in arterial blood pressure is commonly attained by an enhanced cardiac output and/or an increased vascular resistance to blood flow. To test whether the increase of blood pressure was dependent on an enhanced cardiac function, cardiac output was measured by a pressure/volume tetrapolar catheter in anaesthetized *Emilin2* and *Mmrn2* mutant mice and wild-type littermates: cardiac output was similar in both mouse strains (data not shown).

In contrast, vascular resistance was significantly augmented in both *Emilin2* and *Mmrn2* knockout animals (data not shown), thus suggesting that the hypertensive phenotype could be ascribed to particular conditions of the peripheral arterial bed. However, while lack of Multimerin-2 realized a distinctive architecture of resistance vessels with a global reduction of the media cross-sectional area, this was not the case for *Emilin2* mutants, in which the size of the media of mesenteric arteries was comparable to controls (figure 10B). Worth of note, the reduction of the media cross-sectional area in resistance vessels of *Mmrn2* null animals, although significant, was much milder than in *Emilin1* knockout mice (figure 10B) (Zacchigna et al, 2006).

Increased vascular resistance may also be due to abnormal vascular contractility or relaxation. To test this possibility, second branch mesenteric arteries were dissected from *Emilin2* and *Mmrn2* null and wild-type mice, mounted in a micromyograph, and stimulated with vasoactive drugs. Mesenteric vessels of *Emilin2* and *Mmrn2* null mice showed normal endothelium-independent and -dependent relaxation, induced respectively with nitroprusside and acethilcholine (data not shown). Contraction in response to stimulation with angiotensin II was

also comparable to wild-type littermates. However, inactivation of *Mmrn2* increased contraction of mesenteric vessels to phenylephrine, an α1 adrenergic receptor agonist (figure 11B), whereas the response of *Emilin2* null vessels to this drug was normal (figure 11A).

ANALYSIS OF INVOLVEMENT OF TGF-β1 IN *Emilin2* AND *Mmrn2* KNOCKOUT PHENOTYPE

TGF-βs are all synthesized as homodimeric proproteins (proTGF-β); the dimeric propeptides, also known as the LAP, are cleaved from the mature TGF-β dimer by furin-type enzymes (Dubois *et al.*, 1995). Mature TGF-β remains non-covalently associated with LAP in the so-called small latent complex (SLC). This association prevents recognition of TGF-β by its high affinity receptors and further downstream signalling. Liberation of biologically active TGF-β requires its dissociation from LAP in a process termed latent TGF-β activation (Annes *et al.*, 2003). Latent TGF-β is converted into its biologically active form by various mechanisms that involve dissociation of TGF-β from LAP. Proteolysis appears to be the most prominent cellular mechanism of latent TGF-β activation (Annes *et al.*, 2003). Independently from proteolytic cleavage, interaction between LAP and thrombospondin-1 (Murphy-Ullrich and Poczatex, 2000) and the mannose-6-phosphate receptor (Dennis and Rifkin, 1991) promote latent TGF-β activation. Also integrins have been shown to bind to and in several cases to activate latent TGF-β (Wipff *et al.*, 2007; Jenkins *et al.*, 2006; Cambier *et al.*, 2005)

Emilin-1 prevents the processing of proTGF-β1 into LAP and mature TGF-β1, a key event for TGF-β1 availability. Increased TGF-β1 signalling is instrumental for the hypertensive phenotype of *Emilin1* null mice, as suggested by the observation that the reduction of TGF-β1 gene dosage reverts this phenotype (Zacchigna et al., 2006). It was therefore important to find out if Emilin-2 and Multimerin-2 share the same properties in TGF-β1 signalling regulation. In an *in vitro* functional assay, full length Emilin-2 and Multimerin-2 were able to decrease induction of CAGA12-lux reporter triggered by a cotransfected expression plasmid encoding proTGF-$\beta1^{C223S/C225S}$, a mutant protein from which mature active TGF-β1 is constitutively released after furin cleavage (figure 12). This inhibitory effect of the two Emilins on TGF-β1 signalling was linked to the EMI domain, as the sole Emilin-2 or Multimerin-2 EMI domain had activity similar to that of full length proteins. Moreover, the effect was specific, as versions of Emilins lacking the EMI domain were not active.

Since Emilin-2 and Multimerin-2 could interfere with TGF-β1 signalling, it was tested whether their inhibitory activity relied on inhibition of the proteolytic processing of proTGF-β1. HEK293T cells were transfected with plasmids expressing proTGF-β1 alone or in combination with Emilins and proteolysis of the precursor monitored by western blotting on cell extracts. As shown in figure 13, both Emilin-2 and Multimerin-2 potently inhibited the cleavage of proTGF-β1 into LAP (~40 kDa band) and TGF-β1 ligand (~12 kDa band).

In order to understand if activity of Emilins entailed the formation of a molecular complex with proTGF-β1, HEK293T cells were transfected with a proTGF-β1 expression construct alone or in combination with a plasmid directing the expression of Emilin-2 or Multimerin-2 EMI domain on the cell surface (GPI-anchored and FLAG-tagged). Cell lysates were immunoprecipitated with anti-LAP antibody and proteins analyzed in a western blot using an anti-FLAG antibody. As shown in figure 14A and 14B, the EMI domain of both Emilin-2 and Multimerin-2 co-imunoprecipitated with LAP, indicating the existence of a supramolecular complex between Emilins and the TGF-β1 precursor or the SLC.

Together, the functional and biochemical evidence revealed a role for Emilin-2 and Multimerin-2 in the control of TGF-β1 activity that may be functionally relevant in the context of blood vessels. In fact, both *Emilin2* and *Mmrn2* knockout mice have a hypertensive phenotype that, like *Emilin1*, may be caused by increased TGF-β1 availability. If Emilin-2 and Multimerin-2 act within the TGF-β1 pathway to promote hypertension, the reduction of *TGF-β1* gene dosage should attenuate the mutant phenotype. Strikingly, inactivation of one *TGF-β1* allele in *Mmrn2* null animals was sufficient to bring blood pressure levels back to normal (figure 15A). On the contrary, the hypertensive phenotype of *Emilin2* knockout mice was not rescued by the deletion of a single *TGF-β1* allele (figure 15B). Therefore, the development of the hypertensive phenotype in *Emilin2*–/– mice is not linked to the disruption of the interaction of the protein with proTGF-β1.

FUNCTIONAL INTERACTION BETWEEN Emilin-2 AND TGF-β2/3

Different isoforms of TGF-βs are expressed in the cardiovascular system during development (Millan *et al.*, 1991; Molin *et al.*, 2003). Since the vascular phenotype of *Emilin2* null mice could not be explained with an increased TGF-β1 availability, an *in vitro* functional assay suitable to test the activity of Emilin-2 towards TGF-β2 and TGF-β3 was developed. In this

assay, constitutively active forms of proTGF-β must be used to induce CAGA12-lux reporter activity. Consequently, expression plasmids encoding for proTGF-β2$^{C226S/C228S/C229S}$ and proTGF-β3$^{C228S/C230S}$ were created by site directed mutagenesis of cysteines essential for latency. Biological activity of these constructs was tested by cotransfection of HEK293T cells with CAGA12-lux reporter and increasing amount of proTGF-β plasmids. The dose-response titration of luciferase activity as a function of increasing amounts of proTGF-β$^{2C226S/C228S/C229S}$ and proTGF-β3$^{C228S/C230S}$ plasmids indicates that both constructs express a constitutively active growht factor and are therefore suitable for *in vitro* functional assays (figure 16A and 16B). Induction of CAGA12-lux reporter activity by mutant proTGF-β2 and proTGF-β3 was reduced when cotransfected with full-length Emilin-2 (figure. 16C and 16D). However, as for TGF-β1, inactivation of a single TGF-β2 allele did not revert completely the blood pressure of Emilin2–/– mice (figure 17), suggesting that altered TGF-β2 signalling is not (or is not the exclusive) factor responsible for this hypertensive phenotype.

DISCUSSION

Using a genetic approach to understand the role of Emilins, our group has undertaken the targeted inactivation of *Emilin1*, *Emilin2*, *Mmrn1* and *Mmrn2* genes in the mouse. *Emilin1* knockout mice have been most intensely investigated: the homozygous mutant mice are grossly normal and fertile. However, morphological examination at the optical and electron microscopic level has revealed interruptions and irregularity of elastic lamellae of aorta and in skin. These data and the finding that the protein binds to other components of elastic fibers such as Elastin and Fibulin-5 suggest a function of Emilin-1 in elastogenesis (Zanetti *et al.*, 2004). Moreover, analysis of the cardiovascular system has shown that *Emilin1* deficient mice are affected by systemic arterial hypertension caused by a decreased diameter of arterial vessels. This phenotype was linked to an increased TGF-β1 signalling: Emilin-1 through the specific binding to proTGF-β1 precursor prevents its maturation and reduces TGF-β1 availability (Zacchigna *et al.*, 2006).

Subjects of this work are other two members of the Emilin family: Emilin-2 and Multimerin-2. Little is known about these proteins: information about Emilin-2 concerns gene and protein structure (Doliana *et al.*, 2001; Amma *et al.*, 2003; Christian *et al.*, 2001), biosynthesis (Doliana *et al.*, 2001; Christian *et al.*, 2001) and expression (Braghetta *et al.*, 2004; Christian *et al.*, 2001; Leimeister *et al.*, 2002). However, the expression pattern of *Emilin2* was previously analyzed only by *in situ* hybridization and there is not a complete study about the deposition of this extracellular matrix protein in embryonic and adult tissue. One major contribution of the present work is the definition of the expression pattern of Emilin-2 and Multimerin2, an information that is important for the interpretation of the phenotypes obtained with gene targeting experiments.
Immunohistochemical staining confirms previous observations revealing that, during mouse development, Emilin-2 is mainly expressed in the myocardium, but not in endocardium and endothelium of cardiac blood vessels (Braghetta *et al.*, 2004). The data show that the protein is deposited around muscle fibers, In addition, the analysis has identified new locations of Emilin-2 expression, such as blood vessels of the central nervous system and the mesenchyme of different organs as tongue, genital tubercle, intervertebral disks anlage and anterior cranial region. The investigation has also shown previously unknown sites of localization of Emilin-2 in the adult, notably in lymphoid organs. In spleen, Emilin-2 is deposed in the white pulp, whereas in thymus it is present in blood vessels of medullar region and in lymphnodes it is found only in medullary

cords. Finally, the analysis has revealed that the protein is deposited in the interstitial space between muscle fiber of heart and in kidney where it forms thin fibers around tubules of medullary region. Notably, Emilin-2 was not detected in blood vessels of any adult organ, indicating that the protein is expressed at low levels, if not at all, in the vascular system.
As for Multimerin-2, the data confirm the restricted expression in endothelium (Christian *et al.*, 2001; Leimeister *et al.*, 2002; Braghetta *et al.*, 2004) of both large conductance arteries, and small resistance vessels. Yet, new details have been also brought to light, such as the deposition of the protein mainly between the internal elastic lamina and the basal side of endothelial cells.

Given the localization just described, a vascular phenotype was expected in *Mmrn2* knockout mice. Indeed, these animals are hypertensive. Of the two mechanisms that increase blood pressure, (increased cardiac output or to increased vascular resistance), the latter is the one involved in hypertension induced by Multimerin-2 deficiency. Of note, the media cross-sectional area of second branch mesenteric arteries was reduced. Systolic blood pressure of *Mmrn2* null mice was similar to *Emilin1* deficient mice. On the contrary, reduction of media cross-sectional area in resistance vessels is much lower in *Mmrn2* than in *Emilin1* null mice. This result argues against the possibility that increased blood pressure in *Mmrn2*-/- mice is determined by the reduction of the diameter of resistance arteries. It is more likely that the alteration is brought about by the increased contractile response of arterial vessels to stimulation with adrenergic agonists like phenylephrine. Of note, this effect seems to be specific for sympathetic stimuli, as the contractility of *Mmrn2*-/- vessels to angiotensin II was normal. So, an abnormal vascular reactivity to sympathetic stimuli could be the direct cause of the hypertensive phenotype of *Mmrn2* null mice.
Given the pathogenetic role of TGF-β1 in the hypertension of *Emilin1* deficient mice, the implication of this growth factor was also studied in Multimerin-2 deficient animals. *In vitro* experiments established that Multimerin-2, through its EMI domain, inhibits TGF-β1 signalling. This activity could be ascribed to the ability of Multimerin-2 to interact, directly or indirectly is not known at the moment, with proTGF-β1 to form a complex in which processing of the precursor into LAP and mature TGF-β1 is prevented. So, in the absence of Multimerin-2, proTGF-β1 could be easily converted to the SLC and the amount of TGF-β1 available for activation increases. In addition to studies *in vitro*, the relevance of Multimerin-2 as TGF-β1 antagonist was validated *in vivo*: by decreasing the TGF-β1 gene dosage, brings the blood pressure back to normal levels.

Soluble mediators such as TGF-β appear to have an important role in EC interaction with SMC. EC secrete TGF-β in a biologically inactive form that can be further activated (Heydarkhan-Hagvall *et al.,* 2003; Nunes *et al.,* 1996). Multimerin-2 is deposed at the basal side of EC and this location suggests a role for this protein in regulation of TGF-β produced by EC itself. Lack of Multimerin-2 in mice leads to hypertension mediated by an increased contractility of vSMC. Therefore, it could be hypothesized that endothelial cells regulate contractility of vascular smooth muscle cells in response to sympathetic activation. This hypothesis entail a paracrine mechanism in which TGF-β produced by EC had an effect on vSMC. In conclusion, these evidences suggests that EC could regulate contractility of vSMC through paracrine effect of TGF-β. Multimerin2 localized between EC and vSMC could control the amount of TGF-β available to SMC. The deletion of Multimerin2 increase the availability of TGF-β to vSMC that increases their response to sympathic stimulus. TGF-β have also a cytostatic effect on vSMC (Zacchigna *et al.*, 2006); the consequent reduction in vessels size (mild in *Mmrn2* null mice) contribute to the generation of hypertensive phenotype. Moreover, there could be an effect of increased TGF-β1 signalling in EC that, at the moment, remain to be investigated (figure 18).

As for Emilin-2, its biochemical activity seems to be very similar to that of Multimerin-2 and Emilin-1. In fact, evidences *in vitro* indicate that Emilin-2 are able to inhibit TGF-β1 signalling by preventing the processing of proTGF-β1 into LAP and mature TGF-β1 by the formation of a complex with immature proTGF-β1. However, Emilin-2 is not expressed in blood vessels. It was therefore a surprise to find that *Emilin2* null mice are also hypertensive. Two other features should be noted on the *Emilin2* phenotype. The first is that the rise of blood pressure is due to increased vascular peripheral resistance. The second is that the media cross sectional area was not different from that of control mice. These two observations suggest that the augmented blood pressure is totally the consequence of the increased contraction of SMC of resistance vessels. How lack of Emilin-2 brings about this alteration is totally unknown. It is also unknown whether regulation of TGF-β signalling is an important step in the pathogenesis of hypertension induced by Emilin-2 deficiency. In fact, the pressure levels were not significantly altered by the inactivation of a single *TGF-β1* allele *in vivo*. TGF-β1 is not the sole isoform of TGF-β expressed in the cardiovascular system. All three TGF-β isoforms are found in the developing myocardium with a characteristic expression pattern for each cytokine. In arterial vessel wall, TGF-β1 is expressed in the endothelium. TGF-β3 expression overlaps with TGF-β2 from E11.5-

E12.5 onward (Molin et al., 2003; Millan et al., 1991). This is produced by the smooth muscle cells and fibroblasts of tunica media (Molin et al., 2003; Millan et al., 1991) and is present in tunica intima and adventitia at later stages (Pelton et al., 1989). TGF-β3 is expressed in the cardiovascular system but does not produce a specific vascular phenotype when inactivated by gene targeting (Kaartinen et al., 1995; Proetzel *et al.*, 1995). On the contrary, the importance of TGF-β2 in the cardiovascular system is highlighted by the phenotype of null mice that have a spectrum of cardiovascular abnormalities, including double-outlet right ventricle, atrioventricular canal defects and interruption of the aortic arch (Sanford *et al.*, 1997; Bartram *et al.*, 2001; Molin *et al.*, 2002). Therefore the possibility should be considered that Emilin-2 could interfere also with TGF-β2 and TGF-β3 signalling. Through the development of a functional *in vitro* assay, it was demonstrated that Emilin-2 inhibits signalling of these other TGF-β isoforms. The relevance of TGF-β2 in cardiovascular system prompted us to check its implication in hypertensive phenotype of *Emilin2* null mice. However, reduction of *TGF-β2* gene dosage in *Emilin2* null background could not rescue blood pressure to normal level. The implication of TGF-β3 in cardiovascular phenotype of *Emilin2* knockout mice *in vivo* remains to be elucidated. Experiments in mice with inactivation of one *TGF-β3* allele should tell us whether the function of Emilin-2 in the vascular system is linked to extracellular regulation of TGF-β signalling. Alternatively, Emilin2 may regulate the processing of other growth factors of the TGF-β family or act on blood pressure through a mechanism totally different from that of Emilin-1 and Multimerin-2. The former possibility should be considered seriously, as existing evidence indicates that Emilin1 is active not only on TGF-βs, nut also on Nodal and Activins, whereas it does not affect BMP and Wnt signaling (Zacchigna *et al*., 2006).

Alternative mechanisms of explanation of the hypertensive phenotype of *Emilin2* null mice should consider the unique expression pattern of this protein, like its association with myocardial cells in heart, its presence in some mesenchymal cells, its transitory expression in blood vessels of the central nervous system or, finally its localization in lymphoid organs. For example, one hypothesis is that the mature form of TGF-β or some other growth factor regulated by Emilin-2 would constitute a humoral agent responsible for hypertension. Hypertension attributed to increased plasma levels of TGF-β has been described in human (Lijnen et al., 2003). In the absence of Emilin-2, the amount of active TGF-βs would rise at some anatomical locations, for instance in lymphnodes. Once secreted, TGF-β could reach the blood stream and, through this way, diffuse to cells of the whole vascular system. This issue was investigated in unpublished

results by comparing the TGF-β levels in the plasma of mutant and control mice and using parabiosis - that is the union of two living individuals that share a circulatory system - as a way to transfer the phenotype from mutant to normal animals. Experiments of parabiosis display that wild type mice maintained normal systolic blood pressure even when connected to null mice (unpublished data). Therefore the amount of TGF-βs present in plasma is not responsible for the increase of blood pressure of *Emilin2* null mice.

In conclusion, at the moment there is not an explanation of how Emilin-2 regulates blood pressure homeostasis. Future studies will address the relevance of TGF-β3 in cardiovascular phenotype of *Emilin2* null mice, the possible regulation of TGF-β3 signalling by Emilin-2 in blood vessels of the central nervous system where Emilin-2 and TGF-β3 (Munger et al, 2008) are expressed, and the effect of Emilin-2 versus different growth factors expressed in cardiovascular system.

REFERENCES

- Akhurst RJ, Lehnert SA, Faissner A, Duffie E (1990). TGF beta in murine morphogenetic processes: the early embryo and cardiogenesis. *Development* **108**: 645-656.
- Amma LL, Goodyear R, Faris JS, Jones I, Ng L, Richardson G, Forrest D (2003). An emilin extracellular matrix protein identified in the cochlear basilar membrane. *Mol Cell Neurosc* **23:** 460-472.
- Annes JP, Munger JS, Rifkin DB (2003). Making sense of latent TGFβ activation. *J Cell Sci* **116**: 217-224.
- Atsawasuwan P, Mochida Y, Katafuchi M, Kaku M, Fong KSK, Csiszar K, Yamauchi M (2008). Lysyl oxidase binds Transforming Growth Factor-β and regulates its signaling via amine oxidase activity. *J Biol Chem* **283**: 34229-34240.
- Attisano L, Wrana JL, Montalvo E, Massague J (1996). Activation of signalling by the activin receptor complex. *Mol Cell Biol* **16**: 1066-1073.
- Ausubel FM, Brent R, Kingston RE, Moore DD, Smith JA, Seidman JG, et al., (1993). Current Protocols in Molecular Biology. *Wiley, New York*.
- Bartram U, Molin DGM, Wisse LJ, Mohamad A, Sanford LP, Doetschman T, Speer CP, Poelmann RE, Gittenberger-de Groot AC (2001). Double-outlet right ventricle and overriding tricuspid valve reflect disturbances of looping, myocardialisation, endocardial cushion differentiation, and apoptosis in TGF-beta2-knockout mice. *Circulation* **103**: 2745-2752.
- Beck S, Le Good JA, Guzman M, Ben Haim N, Roy K, Beermann F, Constam DB (2002). Extraembryonic proteases regulate Nodal signalling during gastrulation. *Nat Cell Biol* **4**: 981-985.
- Blobe GC, Schiemann WP, Lodish HF (2000). Role of transforming growth factor β in human disease. *N Engl J Med* **342**: 1350-1358.
- Bonaldo P, Braghetta P, Zanetti M, Piccolo S, Volpin D, Bressan GM (1998). Collagen VI deficiency induces early onset myopathy in the mouse: an animal model for Bethlem myopathy. *Hum Mol Genet* **7**: 2135-2140.
- Bornstein P (2001). Thrombospondins as matricellular modulators of cell function. *J Clin Invest* **107**: 929-934.

- Braghetta P, Ferrari A, de Gemmis P, Zanetti M, Volpin D, Bonaldo P, Bressan GM (2004). Overlapping, complementary and site-specific expression pattern of genes of the EMILIN/Multimerin family. *Matrix Biol* **22**: 549-556.
- Bressan GM, Castellani I, Colombatti A, Volpin D (1983). Isolation and characterization of a 115,000 dalton matrix-associated glycoprotein from chick aorta. *J Biol Chem* **258**: 13262-13267.
- Bressan GM, Daga-Gordini D, Colombatti A, Castellani I, Marigo V, Volpin D (1993). Emilin, a component of elastic fibers preferentially located at the elastin-microfibrils interface. *J Cell Biol* **121**: 201-212.
- Cambien F, Ricard S, Troesch A, Mallet C, Générénaz L, Evans A, Arveiler D, Luc G, Ruidavets JB, Poirier O (1996). Polymorphisms of the transforming growth factor-beta 1 gene in relation to myocardial infarction and blood pressure. The Etude Cas-Témoin de l'Infarctus du Myocarde (ECTIM) Study. *Hypertension* **28**: 881-887.
- Cambier S, Gline S, Mu D, Collins R, Araya J, Dolganov G, Einheber S, Boudreau N, Nishimura SL (2005). Integrin alpha(v)beta8-mediated activation of transforming growth factor-beta by perivascular astrocytes: an angiogenic control switch. *Am J Pathol* **166**: 1883-1894.
- Carta L, Pereira L, Arteaga-Solis E, Lee-Arteaga SY, Lenart B, Starcher B *et al.* (2006). Fibrillins 1 and 2 perform partially overlapping functions during aortic development. *J Biol Chem* **281**: 8016-8023.
- Christ M, McCartney-Francis N, Kulkarni AB, Ward JM, Mizel DE, Mackall CL, Gress RE, Hines KL, Tian H, Karlsson S, Wahl SM (1994). Immune dysregulation in TGF-β1 deficient mice. *J Immunol* **153**: 1936-1946.
- Christian S, Ahorn H, Novatchkova M, Garin-Chesa P, Park JE, Weber G, Eisenhaber F, Rettig WJ, Lenter MC (2001). Molecular cloning and characterization of EndoGlyx-1, an EMILIN-like multisubunit glycoprotein of vascular endothelium. *J Biol Chem* **276**: 48588-48595.
- Collod-Beroud G, Boileau C (2002). Marfan syndrome in the third Millennium. *Eur J Hum Genet* **10**: 673-681.
- Colombatti A, Bressan GM, Castellani I, Volpin D (1985). Gp115, a glycoprotein isolated from blood vessels, is widely distributed in connective tissue. *J Cell Biol* **100**: 18-26.
- Colombatti A, Doliana R, Bot S, Canton A, Mongiat M, Mungiguerra G, Paron-Cilli S, Spessotto P (2000). The EMILIN protein family. *Matrix Biol* **19**: 289-301.

- Curran ME, Atkinson DL, Ewart AK, Morris CA, Leppert MF, Keating MT (1993). The elastin gene is disrupted by a translocation associated with supravalvular aortic stenosis. *Cell* **73**: 159-168.
- Dabovic B, Chen Y, Colarossi C, Obata H, Zambuto L, Perle MA, Rifkin DB (2002). Bone abnormalities in latent TGF-[beta] binding protein (Ltbp)-3-null mice indicate a role for Ltbp-3 in modulating TGF-[beta] bioavailability. *J Cell Biol* **156**: 227-232.
- Danussi C, Spessotto P, Petrucco A, Wassermann B, Sabatelli P, Montesi M, Doliana R, Bressan GM, Colombatti A (2008). *Emilin1* deficiency causes structural and functional defects of lymphatic vasculature. *Mol Cell Biol* **28**: 4026-4039.
- Dennis PA and Rifkin DB (1991). Cellular activation of latent transforming growth factor beta requires binding to the cation-independent mannose 6-phosphate/insulin-like growth factor type II receptor. *Proc Natl Acad Sci USA* **88**: 580-584.
- Dickson MC, Martin JS, Cousins FM, Kulkarni AB, Karlsson S, Akhurst RJ (1995). Defective haematopoiesis and vasculogenesis in transforming growth factor β1 knock out mice. *Development* **121**: 1845-1854.
- Doliana R, Mongiat M, Bucciotti F, Giacomello E, Deutzmann R, Volpin D, Bressan GM, Colombatti A (1999). EMILIN, a component of the elastic fiber and a new member of the C1q/tumor necrosis factor superfamily of proteins. *J Biol Chem* **274:** 16773-16781.
- Doliana R, Bot S, Bonaldo P, Colombatti A (2000). EMI, a novel cysteine-rich domain of EMILINs and other extracellular proteins, interacts with the gC1q domains and partecipates in multimerization. *FEBS Lett* **484**: 164-168.
- Doliana R, Bot S, Mungiguerra G, Canton A, Paron Cilli S, Colombatti A (2001). Isolation and characterization of EMILIN-2, a new component of the growing EMILINs family and a member of the EMI domain-containing superfamily. *J Biol Chem* **276**: 12003-12011.
- Drews F, Knöbel S, Moser M, Muhlack KG, Mohren S, Stoll C, Bosio A, Gressner AM, Weiskirchen R (2008). Disruption of the latent transforming growth factor-beta binding protein-1 gene causes alteration in facial structure and influences TGF-beta bioavailability. *Biochim Biophys Acta* **1783**: 34-48.
- Brown CB, Boyer AS, Runyan RB, Barnett JV (1999). Requirement of type III TGF-β receptor for endocardial cell transformation in the heart. *Science* **283**: 2080-2082.

- Dubois CM, Laprise MH, Blanchette F, Gentry LE, Leduc R (1995). Processing of transforming growth factor β1 precursor by human furin convertase. *J Biol Chem* **270**: 10618-10624.
- Fahrenbach WH, Sandberg LB, Cleary EG (1966). Ultrastructural studies on early elastogenesis. *Anat Rec* **155**: 563-576.
- Faury G, Pezet M, Knutsen RH, Boyle WA, Heximer SP, McLean SE, Minkes RK, Blumer KJ, Kovacs A, Kelly DP, Li DY, Starcher B, Mecham RP (2003). Developmental adaptation of the mouse cardiovascular system to elastin haploinsufficiency. *J Clin Invest* **112**: 1419-1428.
- Feng XH, Derynck R (2005). Specificity and versatility in TGF-β signaling through Smads. *Annu Rev Cell Dev Biol* **21**: 659-693
- Franzén P, ten Dijke P, Ichijo H, Yamashita H, Schulz P, Heldin CH, Miyazono K (1993). Cloning of a TGFβ type I receptor that forms a heteromeric complex with the TGFβ type II receptor. *Cell* **75**: 681-692.
- Greenlee TK, Ross R, Hartmann JL (1966). The fine structure of elastic fiber. *J Cell Biol* **30**: 59-71.
- Goumans MJ, Valdimarsdottir G, Itoh S, Rosendahl A, Sideras P, ten Dijke P (2002). Balancing the activation state of the endothelium via two distinct TGF-β type I receptors. *EMBO J* **21**: 1743-1753.
- Goumans MJ, Mummery C (2000). Functional analysis of the TGFβ receptor/Smad pathway through gene ablation in mice. *Int J Dev Biol* **44**: 253-265.
- Habashi JP, Judge DP, Holm TM, Cohn RD, Loeys BL Cooper TK, Myers L *et al.* (2006). Losartan, an AT1 antagonist, prevents aortic aneurysm in a mouse model of Marfan syndrome. *Science* **312**: 117-121.
- Heldin CH, Miyazono K, ten Dijke P (1997). TGF-βsignalling from cell membrane to nucleus through SMAD proteins. *Nature* **390**: 465-471.
- Heydarkhan-Hagvall S, Helenius G, Johansson BR, Li JY, Mattsson E, Risberg B (2003). Co-colture of endothelial cells and smooth muscle cells affects gene expression of angiogenic factors. *J Cell Biochem* **89**: 1250-1259.
- Higuchi R, Krummel B, Saiki RK (1988). A general method of *in vitro* preparation and specific mutagenesis of DNA fragments: study of protein and DNA interactions. *Nucleic Acids Res* **16**: 7351-7367.

- Imamura T, Takase M, Nishihara A, Oeda E, Hanai J, Kawabata M, Miyazono K (1997). Smad6 inhibits signalling by the TGF-β superfamily. *Nature* **389**: 622-626.
- Jenkins RG, Su X, Su G, Scotton CJ, Camerer E, Laurent GJ, Davis GE, Chambers RC, Matthay MA, Sheppard D (2006). Ligation of protease-activated receptor 1 enhances alpha(v)beta6 integrin-dependent TGF-beta activation and promotes acute lung injury. *J Clin Invest* **116**: 1606-1614.
- Judge DP, Dietz HC (2005). Marfan's syndrome. *Lancet* **366**: 1965-1976.
- Kaartinen V, Voncken JW, Shuler C, Warburton D, Bu D, Heisterkamp N, Groffen J (1995). Abnormal lung development and cleft palate in mice lacking TGF-β3 indicates defects of epithelial-mesenchymal interactions. *Nat Genet* **11**: 415-421.
- Karnik SK, Brooke BS, Bayes-Genis A, Sorensen L, Wythe JD, Schwartz RS, Keating MT, Li DY (2003). A critical role for alastin signaling in vascular morphogenesis and disease. *Development* **130**: 411-423.
- Kulkarni AB, Huh C, Becker D, Geiser A, Lyght M, Flanders KC, Roberts AB, Sporn MB, Ward JM (1993). Transforming growth factor β1 null mutation in mice causes excessive inflammatory response and early death. *Proc Natl Acad Sci USA* **90**: 770-774.
- Larrain J, Bachiller D, Lu B, Agius E, Piccolo S, De Robertis EM (2000). BMP-binding modules in chordin: a model for signalling regulation in the extracellular space. *Development* **127**: 821-830.
- Lebrin F, Goumans MJ, Jonker L, Carvalho RL, Valdimarsdottir G, Thorikay M, Mummery C, Arthur HM, ten Dijke P (2004). Endoglin promotes endothelial cell proliferation and TGF-beta/ALK1 signal transduction. *EMBO J* **23**: 4018-4028.
- Leimeister C, Steidl C, Schumacher N, Erhard S, Gessler M (2002). Developmental expression and biochemical characterization of Emu family members. *Dev Biol* **249**: 204-218.
- Lembo G, Vecchione C, Fratta L, Marino G, Trimarco V, d'Amati G, Trimarco B (2000). Leptin induces direct vasodilation through distinct endothelialmechanisms. *Diabetes* **49**: 293-297.
- Li DY, Brooke B, Davis EC, Mecham RP, Sorensen LK, Boak BB, Eichwald E, Keating MT (1998a). Elastin is an essential determinant of arterial morphogenesis. *Nature* **393**: 276-280.

- Li DY, Faury G, Taylor DG, Davis EC, Boyle WA, Mecham RP, Stenzel P, Boak B, Keating MT (1998b). Novel arterial pathology in mice and humans hemizygous for elastin. *J Clin Invest* **102**: 1783-1787.
- Lijnen PJ, Petrov VV, Fagard RH (2003). Association between transforming growth factor-beta and hypertension. *Am J Hypertens* **16**: 604-611.
- Massague J, Gomis RR (2006). The logic of TGFβ signaling. *FEBS Lett* **580**: 2811-2820.
- Millan FA, Denhez F, Kondaiah P, Akhurst RJ (1991). Embryonic gene expression pattern of TGF beta1, beta2 and beta3 suggest different developmental function in vivo. *Development* **111**: 131-144.
- Miyazono K, Olofsson A, Colosetti P, Heldin CH (1991). A role of the latent TGF-β-binding protein in the assembly and secretion of TGF-β. *EMBO J* **10:** 1091-2101.
- Molin DGM, DeRuiter MC, Wisse LJ, Azhar M, Doetschman T, Poelmann RE, Gittenberger-de Groot AC (2002). Altered apoptosis pattern during pharyngeal arch artery remodelling is associated with aortic arch malformations in *Tgf*β*2* knock-out mice. *Cardiovasc Res* **56**: 312-322.
- Molin DG, Bartram U, Van der Heiden K, Van Iperen L, Speer CP, Hierck BP, Poelmann RE, Gittenberg-de-Groot AC (2003). Expression patterns of TGFβ 1-3 associate with myocardialisation of the outflow tract and the development of the epicardium and the fibrous heart skeleton. *Dev Dyn* **227**: 431-444.
- Mongiat M, Mungiguerra G, Bot S, Mucignat MT, Giacomello E, Doliana R, Colombatti A (2000). Self-assembly and supramolecular organization of EMILIN. *J Biol Chem* **275**: 25471-25480.
- Mongiat M, Ligrasti G, Marastoni S, Lorenzon E, Doliana R, Colombatti A (2007). Regulation of the extrinsic apoptotic pathway by the extracellular matrix glycoprotein EMILIN2. *Mol Cell Biol* **27**: 7176-7187.
- Mu Z, Yang Z, Yu D, Zhao Z, Munger JS (2008). TGFβ1 and TGFβ3 are partially redundant effectors in brain vascular morphogenesis. *Mech Dev* **125**: 508-516.
- Murphy-Ullrich JE and Poczatek M (2000). Activation of latent TGF-beta by thrombospondin-1: mechanisms and physiology. *Cytokine Growth Factor Rev* **11**: 59-69.
- Müller U (1999). Ten years of gene targeting: targeted mouse mutants, from vector design to phenotype analysis. *Mech Dev* **82**: 3-21.

- Nagy A, Gertsenstein M, Vinterstein K, Behringer R. Manipulation the mouse embryo-A laboratory manual-Third edition. Cold Spring Harbor Laboratory Press, 2003.
- Nakao A, Afrakhte M, Morn A, Nakayama T, Christian JL, Heuchel R, Itoh S, Kawabata M, Heldin NE, Heldin CH, ten Dijke P (1997). Identification of Smad7, a TGF-β inducible antagonist of TGF-β signalling. *Nature* **389**: 631-635.
- Neptune ER, Frischmeyer PA, Arking DE, Myers L, Bunton TE, Gayraud B, Ramirez F, Sakai LY, Dietz HC (2003). Dysregulation of TGF-beta activation contributes to pathogenesis in Marfan syndrome. *Nat Genet* **33**: 407-411.
- Nunes I, Gleizes PE, Metz CN, Rifkin DB (1997). Latent transforming growth factor-β binding protein domains involved in activation and transglutaminasedependent cross-linking of latent transforming growth factor-β. *J Cell Biol* **136**: 1151-1163.
- Nunes I, Munger JS, Harpel JG, Nagano Y, Shapiro RL, Gleizes PE, Rifkin DB (1996). Structure and activation of the large latent transforming growth factor-beta complex. *Int J Obes Relat Metab Disord* **20 Suppl 3**: S4-S8.
- O'Reilly MS, Boehm T, Shing Y, Fukai N, Vasios G, Lane WS, Flynn E, Birkhead JR, Olsen BR, Folkman J (1997). Endostatin: an endogenous inhibitor of angiogenesis and tumor growth. *Cell* **88**: 277-285.
- Pelton RW, Nomura S, Moses HL, Hogan BL (1989). Expression of transforming growth factor beta 2 RNA during murine embryogenesis. *Development* **106**: 759-767.
- Proetzel G, Pawlowski SA, Wiles MV, Yin M, Boivin GP, Howles PN, Ding J, Ferguson MWJ, Doetschmann T (1995). Transforming gorwth factor-β3 is required for secondary palate fusion. *Nat Genet* **11**: 409-414.
- Rifkin DB (2005). Latent transforming growth factor-β (TGF-β) binding proteins: orchestrators of TGF-β availability. *J Biol Chem* **280**: 7409-7412.
- Saharinen J, Taipale J, Keski-Oja J (1996). Association of the small latent transforming growth factor-β with an eight cysteine repeat of its binding protein LTBP-1. *EMBO J.* **15**: 245-253.
- Saharinen J, Keski-Oja J (2000). Specific sequence motif of 8-Cys repeats of TGF-β binding proteins, LTBPs, creates a hydrophobic interaction surface for binding of small latent TGF-β. *Mol Biol Cell* **11**: 2691-2704.
- Sakai LY, Keene DR, Engvall E (1986). Fibrillin, a new 350-kD glycoprotein, is a component of extracellular microfibrils. *J Cell Biol* **103**: 2499-2509.

- Sambrook J, Fritsch EF, Maniatis T. Molecular cloning-A laboratory manual-Second edition. Cold Spring Harbor Laboratory Press, 1989.
- Sanford LP, Ormsby I, Gittenberger-deGroot AC, Sariola H, Friedman R, Boivin JP, Cardell EL, Doetschman T (1997). TGFbeta2 knockout mice have multiple developmental defects that are non-overlapping with other TGFbeta knockout phenotypes. *Development* **124**: 2659-2670.
- Sanz-Moncasi MP, Garin-Chesa P, Stockert E, Jaffe EA, Old LJ, Rettig WJ (1994). Identification of a high molecular weight endothelial cell surface glycoprotein, endoglyx-1, in normal and tumor blood vessels. *Lab Invest* **71**: 366-373.
- Schmierer B, Hill CS (2007). TGFβ-SMAD signal transduction: molecular specificity and functional flexibility. *Nat Rev Mol Cell Biol* **8**: 970-982.
- Shi Y, Massagué J (2003). Mechanisms of TGF-β signalling from cell membrane to nucleus. *Cell* **113**: 685-700.
- Shull MM, Ormsby I, Kier AB, Pawlowsky S, Diebold RJ, Yin M, Allen R, Sidman C, Preotzel G, Calvin D, Ammunziata N, Doetschman T (1992). Target disruption of the mouse transforming growth factor-β1 gene results in multifocal inflammatory disease. *Nature* **359**: 693-699.
- Sinha S, Nevett C, Shuttleworth CA, Kielty CM (1998). Cellular and extracellular biology of the latent transforming growth factor-beta binding proteins. *Matrix Biol* **17**: 529-545
- Spessotto P, Cervi M, Mucignat MT, Mungiguerra G, Sartoretto I, Doliana R, Colombatti A (2003). β_1 integrin-dependent cell adhesion to EMILIN-1 is mediated by the gC1q domain. *J Biol Chem* **278**: 6160-6167.
- Souchelnytskyi S, Tamaki K, Engström U, Wernstedt C, ten Dijke P, Heldin CH (1997). Phosphorylation of Ser465 and Ser467 in the C terminus of Smad2 mediates interaction with Smad4 and is required for transforming growth factor-β signaling. *J Biol Chem* **272**: 28107-28115.
- Sterner-Kock A, Thorey IS, Koli K, Wempe F, Otte J, Bangsow T, Kuhlmeier K, Kirchner T, Jin S, Keski-Oja J, von Melchner H (2002). Disruption of the gene encoding the latent transforming growth factor-beta binding protein 4 (LTBP-4) causes abnormal lung development, cardiomyopathy, and colorectal cancer. *Genes Dev* **16**: 2264-2273.

- Strausberg RL, Feingold EA, Grouse LH, Derge JG, Klausner RD, Collins FS et al. (2002). Generation and initial analysis of more than 15000 full length human and mouse cDNA sequences. *Proc Natl Acad Sci USA* **99**: 16899-16903.
- Suthanthiran M, Li B, Song JO, Ding R, Sharma VK, Schwartz JE, August P (2000). Transforming growth factor-β_1 hyperexpression in african-american hypertensives: a novel mediator of hypertension and/or target organ damage. *Proc Natl Acad Sci USA* **97**: 3479-3484.
- Taipale J, Keski-Oja J (1997). Growth factors in the extracellular matrix. *FASEB J* **11**: 51-59.
- ten Dijke P, Arthur HM (2007). Extracellular control of TGFβ signalling in vascular development and disease. *Nat Rev Mol Cell Biol* **8**: 857-869.
- Vecchione C, Fratta L, Rizzoni D, Notte A, Poulet R, Porteri E, Frati G, Guelfi D, Trimarco V, Mulvany MJ, Agabiti-Rosei E, Trimarco B, Cotecchia S, Lembo G (2002). Cardiovascular influences of alpha1b-adrenergic receptor defect in mice. *Circulation* **105**: 1700-1707.
- Wood JR, Bellamy D, Child AH, Citron KM (1984). Pulmonary disease in patients with Marfan syndrome. *Thorax* **39**: 780-784.
- Wrana JL, Attisano L, Wieser R, Ventura F, Massague J (1994) Mechanism of activation of the TGF-β receptor. *Nature* **370**: 341-347.
- Wipff PJ, Rifkin DB, Meister JJ, Hinz B (2007). Myofibroblast contraction activates TGFβ1 from the extracellular matrix. *J Cell Biol* **179**. 1311-1323.
- Yanagisawa H, Davis EC, Starcher BC, Ouchi T, Yanagisawa M, Richardson JA, Olson EN (2002). Fibulin-5 is an elastin-binding protein essential for elastic fibre development in vivo. *Nature* **415**: 168-171.
- Zacchigna L, Vecchione C, Notte A, Maretto S, Cifelli G, Dupont S, Ferrari A, Maffei A, Marino G, Cordenonsi M, Selvetella G, Aretini A, Colonnese C, Bettarini U, Russo G, Fabbro C, Soligo S, Adorno M, Braghetta P, Bonaldo P, Volpin D, Piccolo S, Lembo G, Bressan GM (2006). Emilin1 links TGF-β maturation to blood pressure homeostasis. *Cell* **124**: 929-942.
- Zamir E, Geiger B (2001). Molecular complexity and dynamics of cell-matrix adhesions. *J Cell Sci* **114**: 3583-3590.

- Zanetti M, Braghetta P, Sabatelli P, Mura I, Doliana R, Colombatti A, Volpin D, Bonaldo P, Bressan GM (2004). EMILIN-1 deficiency induces elastogenesis and vascular cell defects. *Mol Cell Biol* **24**: 638-650.
- Zhang H, Apfelroth SD, Hu W, Davis EC, Sanguineti C, Bonadio J, Mecham RP, Ramirez F (1994). Structure and expression of fibrillin-2, a novel microfibrillar component preferentially located in elastic matrices. *J Cell Biol* **124**: 855-863.
- Zhu Y, Oganesian A, Keene DR, Sandell LJ (1999). Type IIA procollagen containing the cysteine-rich amino propetide is deposited in the extracellular matrix of prechondrogenic tissue and binds to TGF-β1 and BMP-2. *J Cell Biol* **144**: 1069-1080.

FIGURES

Figure 1: The EDEN (EMI domain endowed) gene superfamily.

EDEN superfamily is characterized by the presence of the N-terminal EMI-domain. The superfamily is composed by three families: Emilins/Multimerins that share, besides EMI domain, the central coiled coil region and the C-terminal gC1q domain; the only member of the truncated Emilin familyin mammals is *Emilin3*, that lacks the gC1q domain; members of Emid family share with other EDEN proteins the sole EMI domain.

THE EDEN SUPERFAMILY

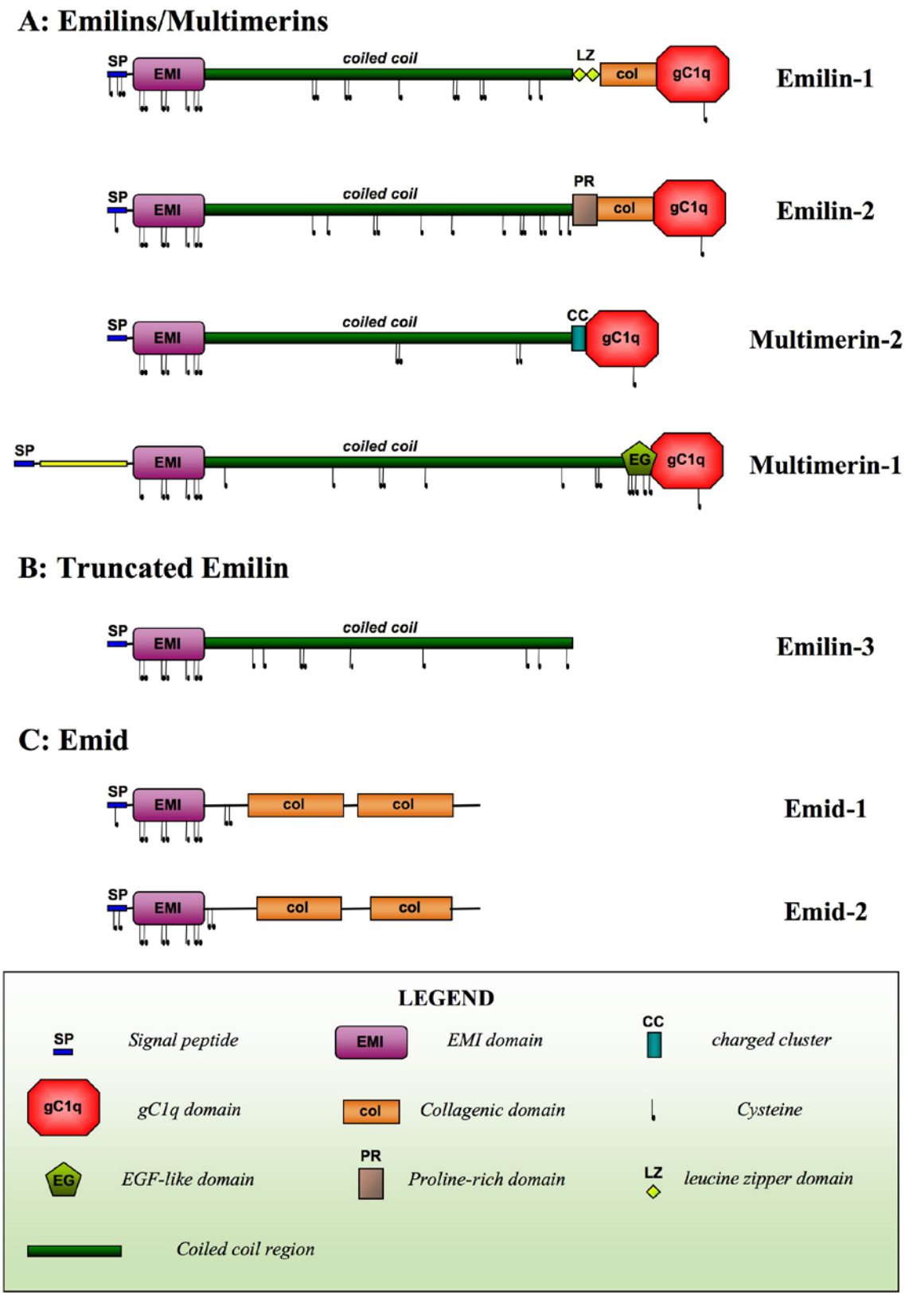

Figure 2: Emilin-2 distribution in the embryo.

A: immunoperoxidase of sagittal section from E13.5 embryo. Emilin-2 is mainly expressed in the heart (arrow), but it is also present in tail mesenchyme (black arrowhead) and in mesenchymal condensations of anterior cranial region (blue arrowhead), genital tubercle (red arrowhead) and tongue (green arrowhead).

B: detection of Emilin-2 in the central nervous system by immunoperoxidase: the protein is deposited in the wall of blood vessels (arrows).

C: immunofluorescence against Emilin-2 in embryonic heart section (E13.5). Emilin-2 is located around muscular fibers in myocardium.

D: immunofluorescence on section of embryonic heart (E13.5). Emilin-2 distribution (green staining) is not coincident with the endothelial specific marker PECAM (red staining).

Bar: in A = 1mm; in B, C and D = 50 μm

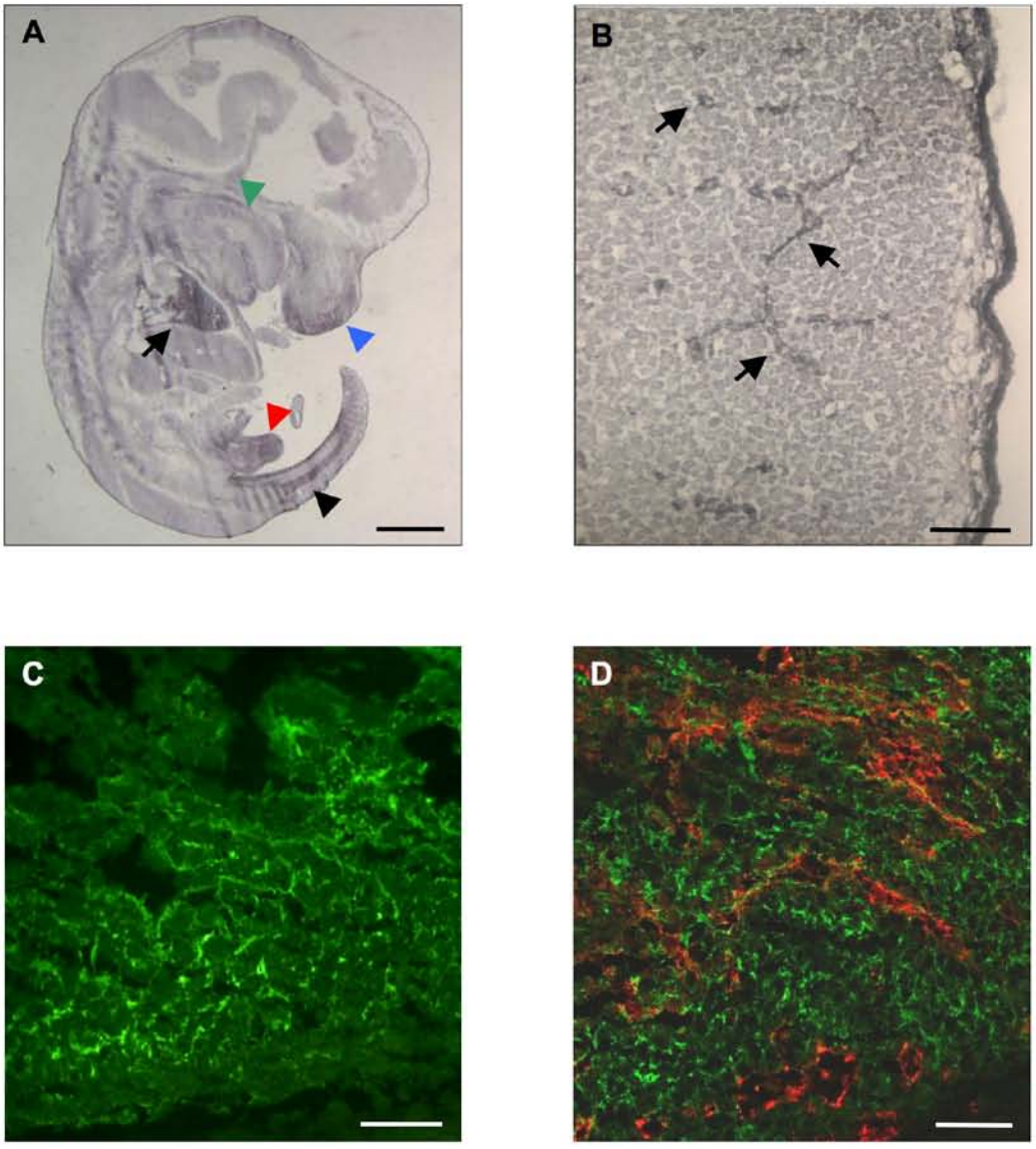
A
B
C
D

Figure 3: Immunoperoxidase staining of Emilin-2 in adult organs.

A: spleen. Staining is present in the white pulp where it forms a thin network around central arterioles. RP: red pulp; WP: white pulp; CA: central arteriole.

B: thymus. Emilin-2 deposition is mainly associated with large blood vessels of medullar region. M: medullar region; C: cortical region.

C, D: lymphnode. Arrows indicate deposition of Emilin-2 in medullar cords. LF: lymphatic follicle; S: medullar sinuses.

E: heart. Staining (arrows) is present between muscle fibers.

F: kidney: Arrow indicates deposition of Emilin-2 between tubules. T: tubule

Bar: in A, B and C = 200 μm; E = 100 μm; D, F = 50 μm.

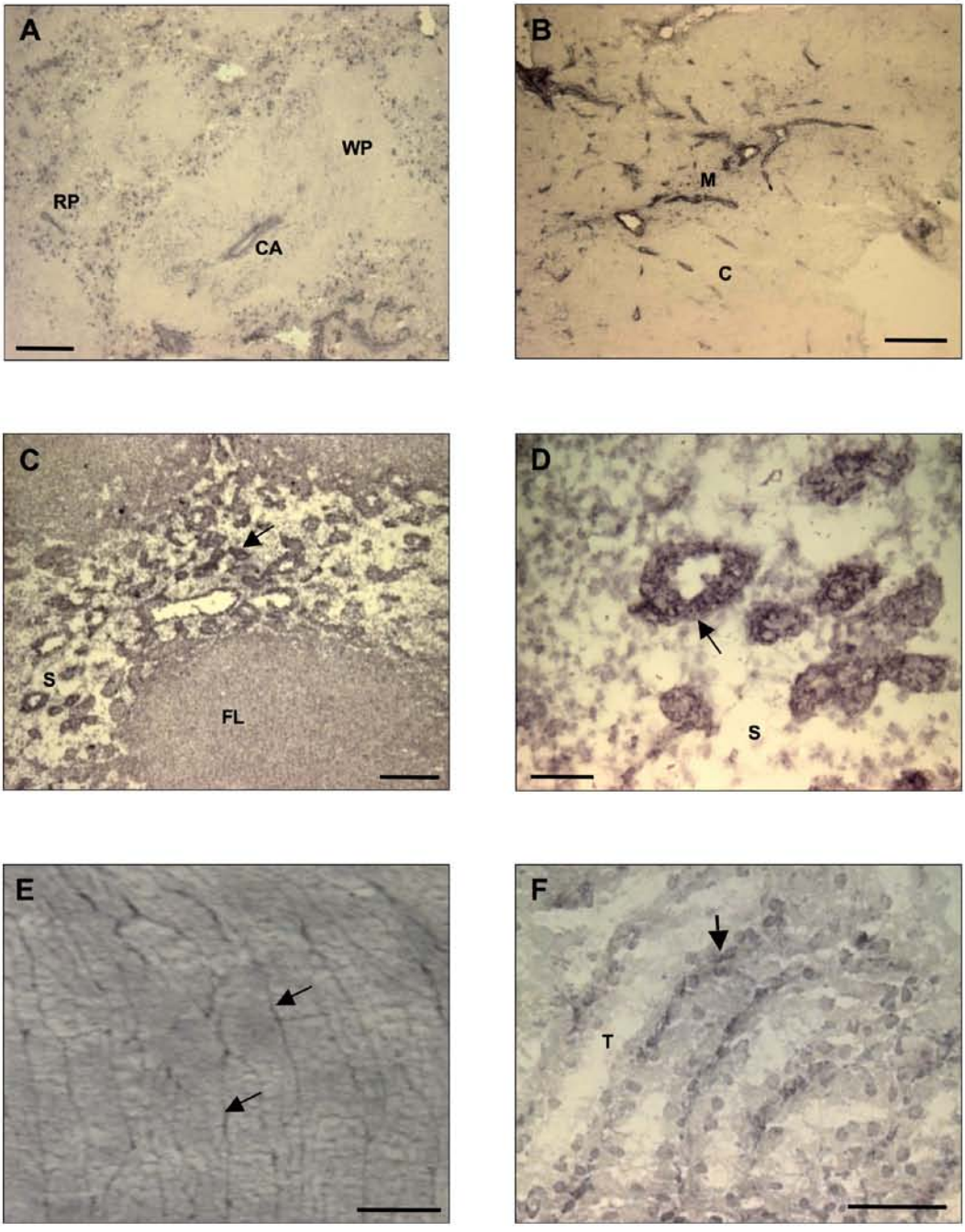
A
WP
RP
CA
B
M
C
C
S
FL
D
S
E
F
T

Figure 4: Immunofluorescence analysis of Multimerin-2 in adult blood vessels.

Multimerin-2 (green staining) expression is restricted to endothelium in aorta, a large conductance artery (**A**) and in resistance vessels like second branch mesenteric arteries (**B**). The internal elastic lamina (asterisks) can be appreciated as a thin rim of autofluorescence just outside Multimerin-2 staining. Nuclei (red) were labelled with propidium iodide. Bar: in A = 100 μm and in B = 10 μm.

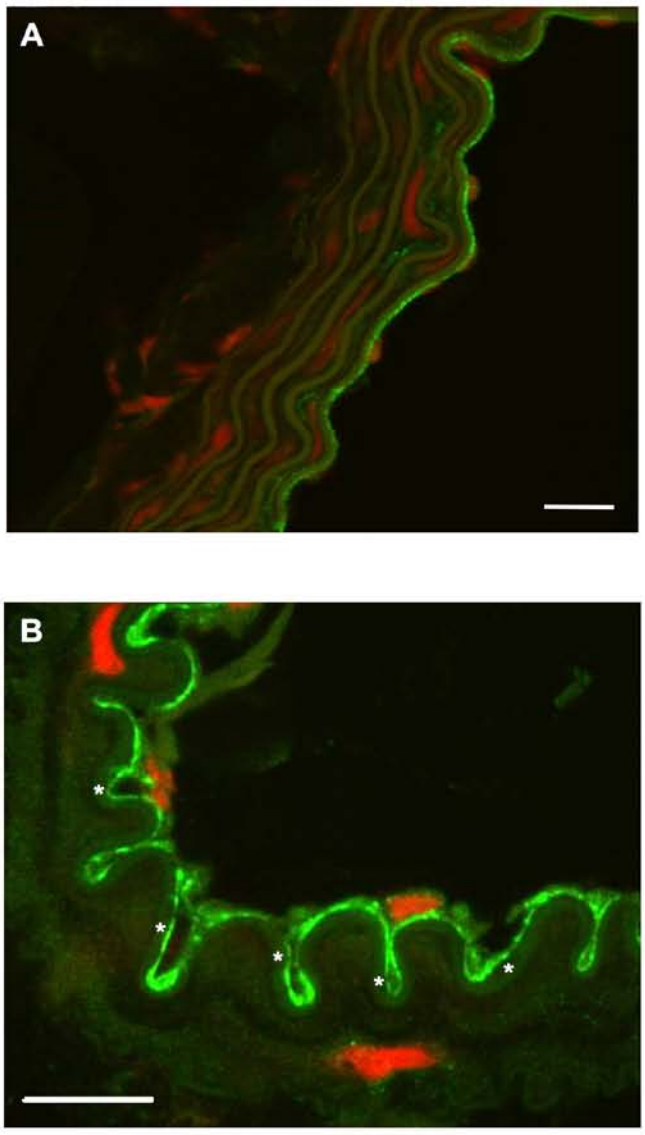
A
B

Figure 5: Strategy of *Emilin2* and *Mmrn2* gene locus targeting.

In targeting vector for *Emilin2* (**A**) the PGK-neo^R cassette was inserted in forward orientation in HindII and NarI sites flanking exon2. A thymidine kinase (TK) cassette was ligated at the 5'-end of the construct for negative selection. In *Mmrn2* targeting vector (**B**) exon1 was replaced with PGK-neo^R cassette inserted in reverse orientation between BglII sites. At the 5' end the construct presents TK cassette.

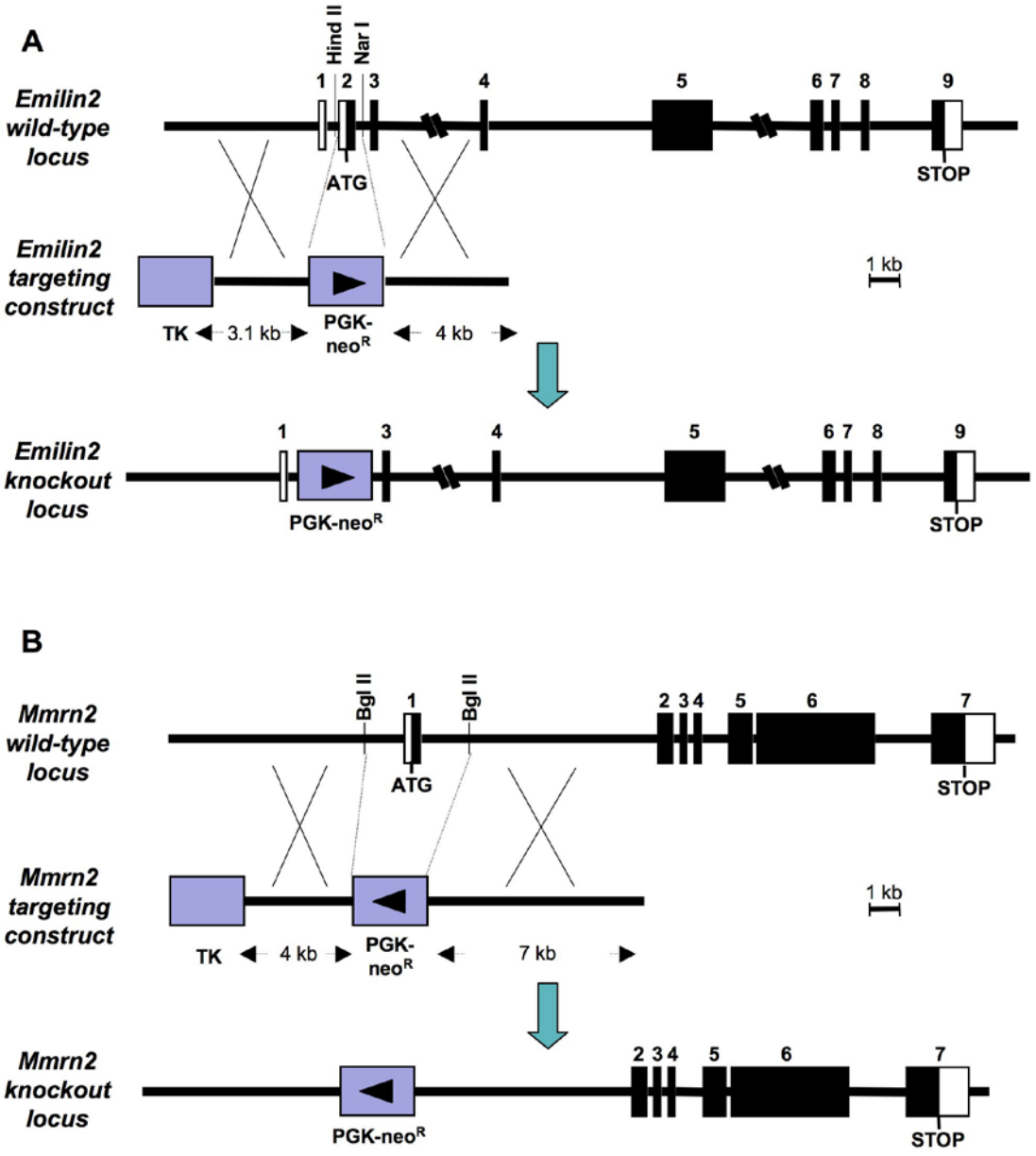
A
Hind II
Nar I
Emilin2 wild-type locus
1 2 3 4 5 6 7 8 9
ATG
STOP
Emilin2 targeting construct
1 kb
TK
3.1 kb
PGK-neoR
4 kb
Emilin2 knockout locus
1 3 4 5 6 7 8 9
PGK-neoR
STOP
B
Mmrn2 wild-type locus
Bgl II
Bgl II
1 2 3 4 5 6 7
ATG
STOP
Mmrn2 targeting construct
1 kb
TK
4 kb
PGK-neoR
7 kb
Mmrn2 knockout locus
2 3 4 5 6 7
PGK-neoR
STOP

Figure 6: Analysis of mRNA from *Emilin2* wild-type and null mice.

A: northern blotting analysis for *Emilin2* on total mRNA from wild-type and null whole embryos revealed the presence of two transcripts of 5.6 and 4.2 kb in mutant mice and a single transcript of 4.5 kb in controls.

B: scheme of primers used in RT-PCR analysis.

C-P: gel-electrophoresis of RT-PCR products from *Emilin2* wild-type and knockout mice.

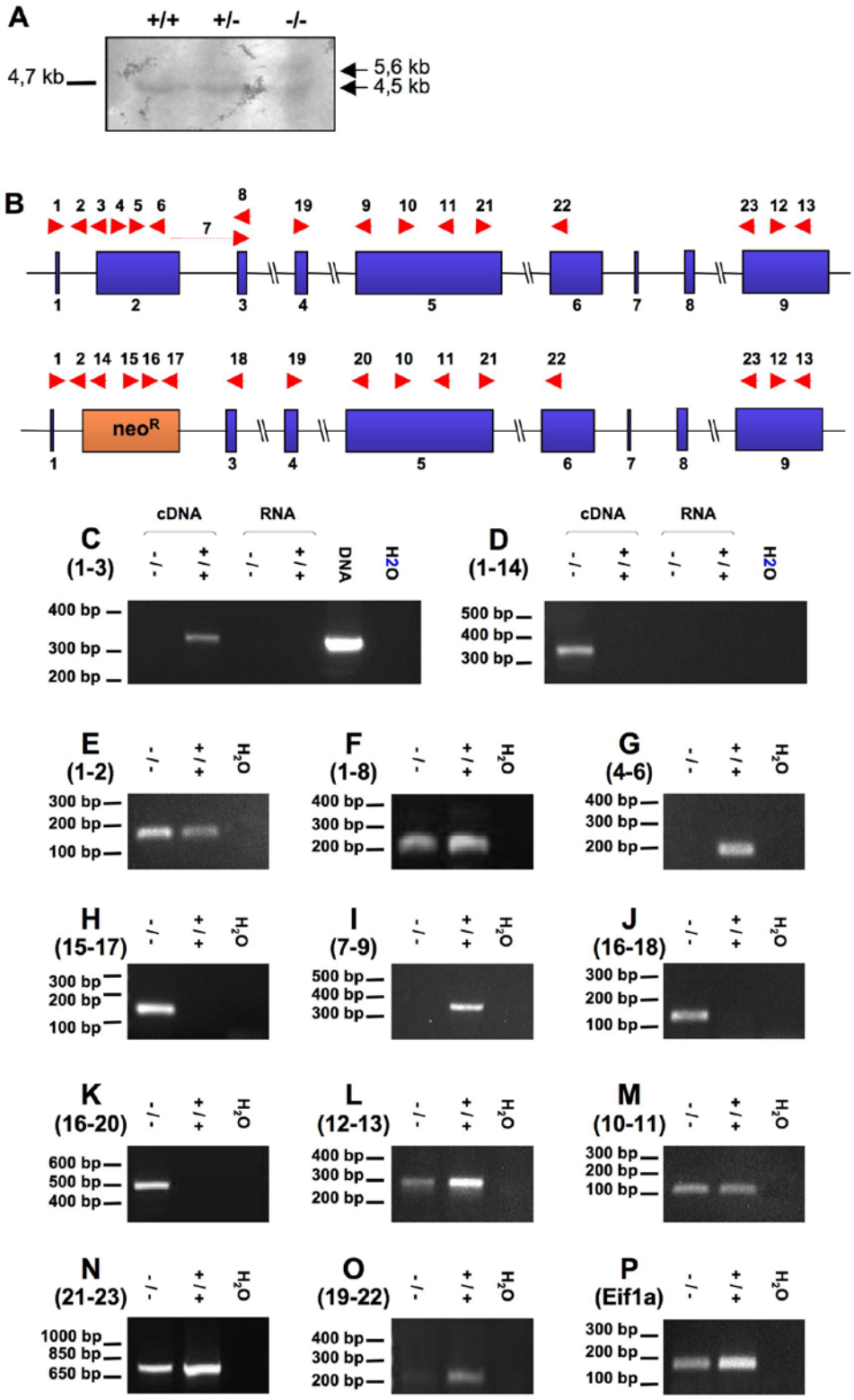
A
+/+
+/-
-/-
4,7 kb
5,6 kb
4,5 kb
B
neoR
C
(1-3)
cDNA
RNA
DNA
H2O
400 bp
300 bp
200 bp
D
(1-14)
500 bp
400 bp
300 bp
E
(1-2)
100 bp
F
(1-8)
G
(4-6)
H
(15-17)
I
(7-9)
J
(16-18)
K
(16-20)
600 bp
500 bp
L
(12-13)
M
(10-11)
N
(21-23)
1000 bp
850 bp
650 bp
O
(19-22)
P
(Eif1a)

Figure 7: Analysis of transcripts from *Emilin2* knockout mice.

A: sequence of RT-PCR product (primers 1-8) derived from knockout mice mRNA. Red = exon 1; Black = 5'-end of intron1; Blue = exon3.

B: structure of the mature transcripts of *Emilin2* wild-type (I-III) and null (IV-VI) animals deduced from RT-PCR analysis. Transcripts with length corresponding to the bands detected in the northern blot are indicated with asterisks.

A

GTTCAAGCCG TGTACTAGCT GCGCCTAGGA GAGCTCCTGC GTCTTCAACT
TTCGCCCAAG ACCTTAAAGA TTGATGGGTA GACGGCGGTG GGGCCTCAGA
GGAAGAAATC GACGCTGAGT CCCCCTTGAA AACTGGTGCG CCTACATCGT
GAATAAGAAC GTGAGCTGCA CGGTACAGGA GGGAAGCGAG AGTTTTATTC
AAGCTCAGTA CAACTGTCCC TGGAACCAGA TG

B

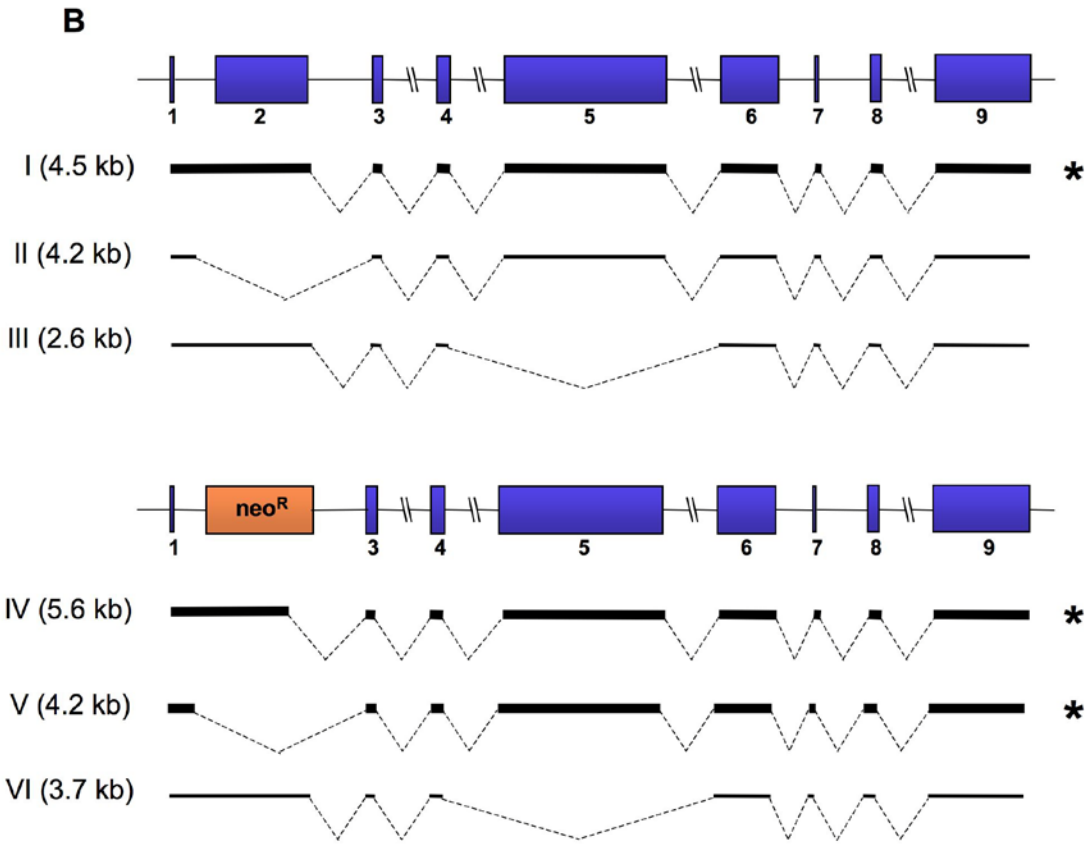

Figure 8: Emilin-2 is absent in knockout animals.

Immunoperoxidase of embrionic heart (**A-B**), spleen (**C-D**), thymus (**E-F**) and lymphnode (**G-H**) from wild-type and knockout mice. Staining for Emilin-2 is not present in sections from null mice, a confirmation of the absence of Emilin-2. Arrows indicate Emilin-2 staining in lymphnode medulle cords. RP: red pulp; WP: white pulp; CA: central arteriole; M: medullar region; C: cortical region; S: medullar sinuses.

Bar: A-B = 200 μm; C-H = 50 μm.

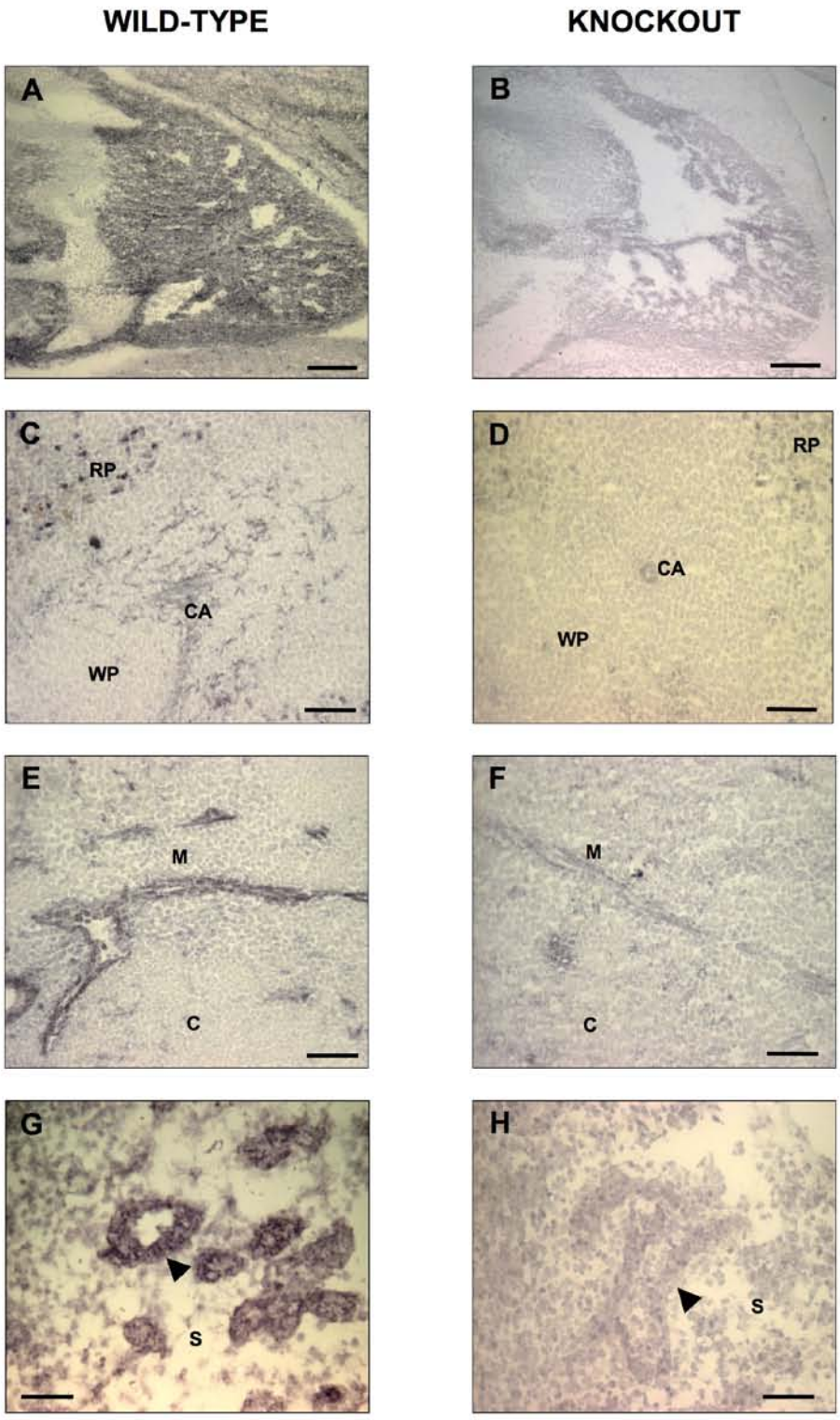
WILD-TYPE
KNOCKOUT
A
B
C
RP
CA
WP
D
RP
CA
WP
E
M
C
F
M
C
G
S
H
S

Figure 9: Analysis of *Mmrn2* gene products.

A: RT-PCR analysis of *Mmrn2* wild type and null mice mRNA with primers amplifying exon1. Multimerin-2 mRNA was absent in null mice.

B: Immunofluorescence against Multimerin-2 in sections of aorta from wild-type and knockout mice confirmig the lack of protein expression in null mice. Arrows = internal elastic lamina. Bar: 10 μm.

C: Western blot on aorta extracts from *Mmrn2*mutant mice. Expression of the protein was completely abolished in knockout animals while it was lower in heterozygous mice.

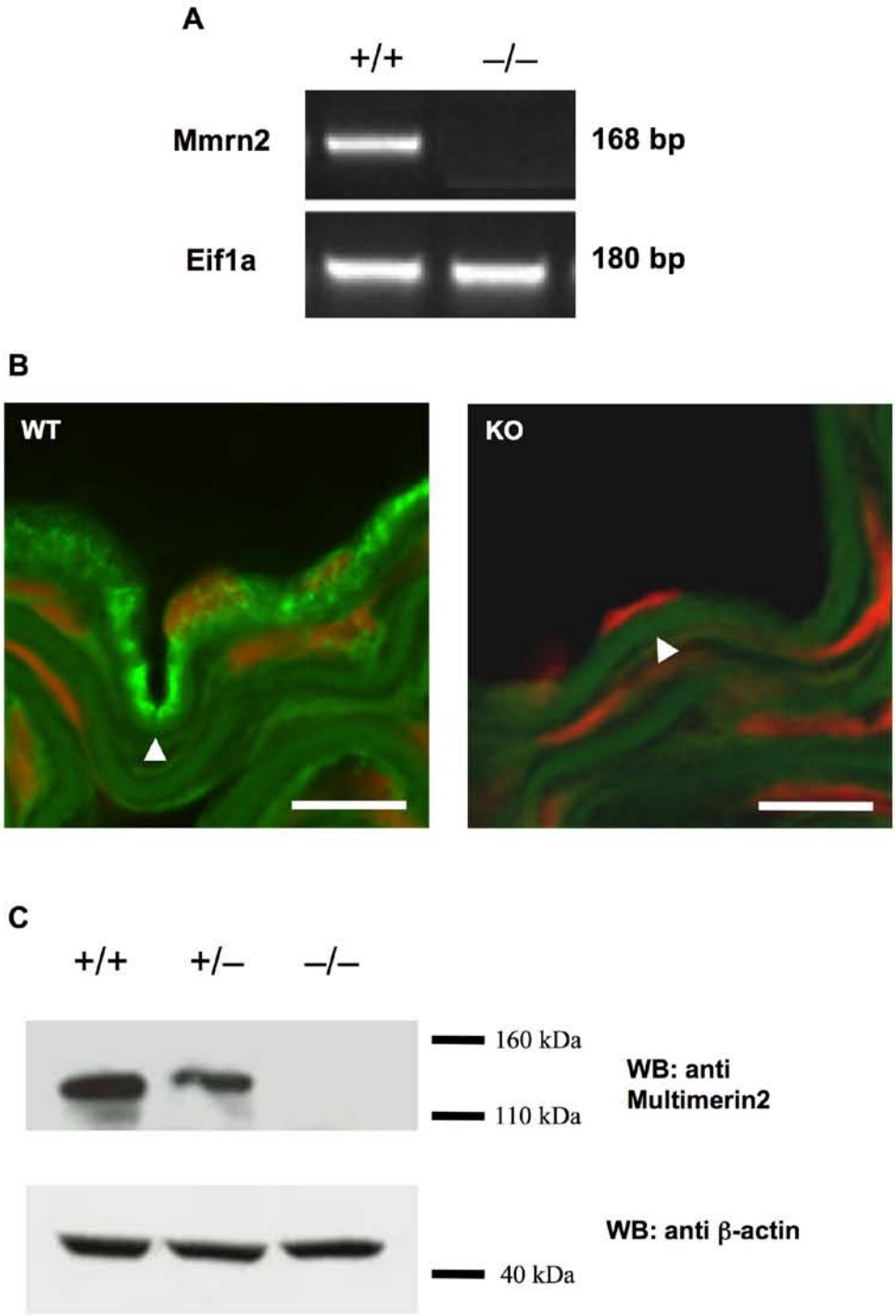
A
+/+
–/–
Mmrn2
168 bp
Eif1a
180 bp
B
WT
KO
C
+/+
+/–
–/–
160 kDa
110 kDa
WB: anti Multimerin2
WB: anti β-actin
40 kDa

Figure 10: Characterization of the vascular phenotype of *Emilin2* and *Mmrn2* null mice.

A: Systolic blood pressure evaluated in wild type and *Emilin1*-/-, *Emilin2*-/- and *Mmrn2*-/- mice non-invasively by tail-cuff plethysmography (n = 6 per group). *$p < 0.05$ versus wild-type mice. Data are mean ±SEM.

B: Analysis of media cross-sectional area (MCSA) in mesenteric arteries from wild type and mutant mice evaluated using a Mulvany myograph (n = 5 for each genotype). * $p < 0.05$ versus wild-type mice. Data are mean ± SEM.

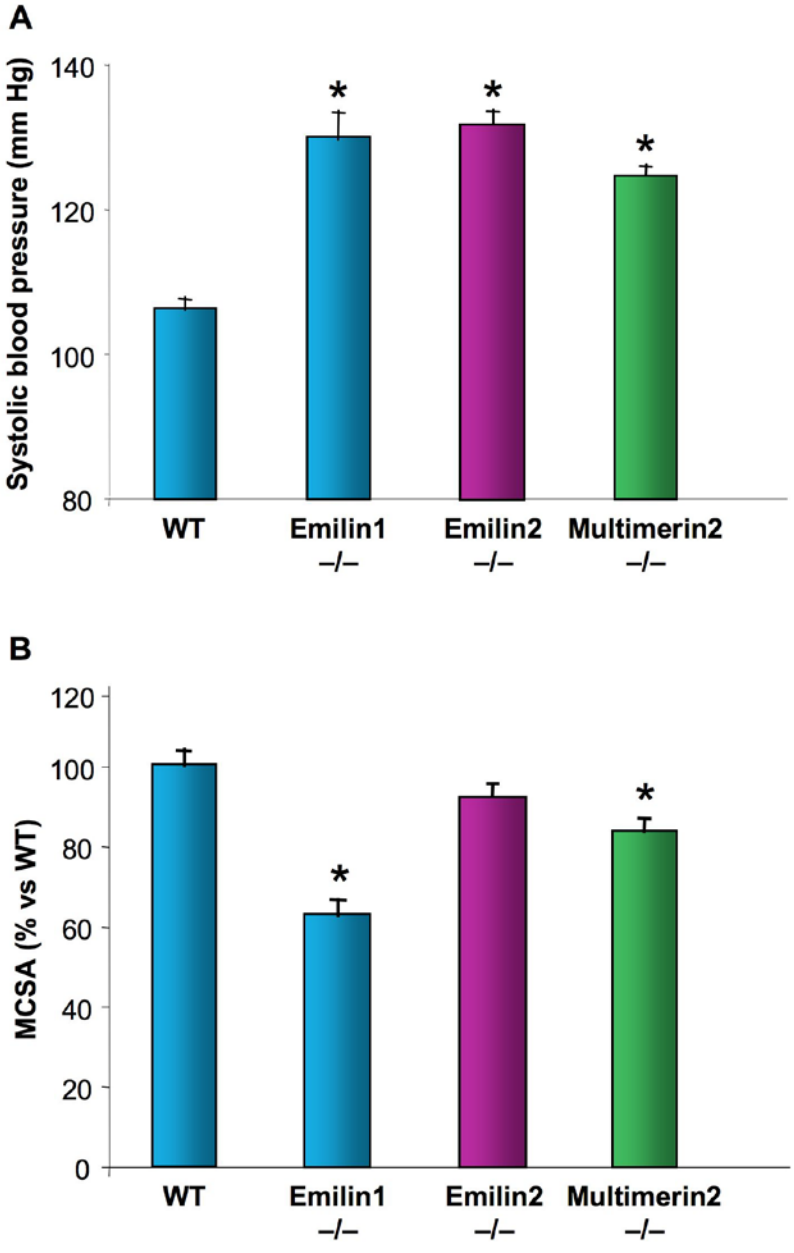
A
Systolic blood pressure (mm Hg)
140
120
100
80
*
*
*
WT
Emilin1 –/–
Emilin2 –/–
Multimerin2 –/–
B
MCSA (% vs WT)
120
100
80
60
40
20
0
*
*
WT
Emilin1 –/–
Emilin2 –/–
Multimerin2 –/–

Figure 11: Inactivation of *Mmrn2* increases response of blood vessels to phenylephrine.
Representative diagram of vascular contraction to phenylephrine in mesenteric arteries from *Emilin2* (**A**) and *Mmrn2* (**B**) null mice. Blue diamonds = wild-type mice; Purple squares = null mice (n = 6 per group). The response of the *Mmrn2* deficient vessels was higher than that elicited in controls, whereas *Emilin2* null mice had a normal response.

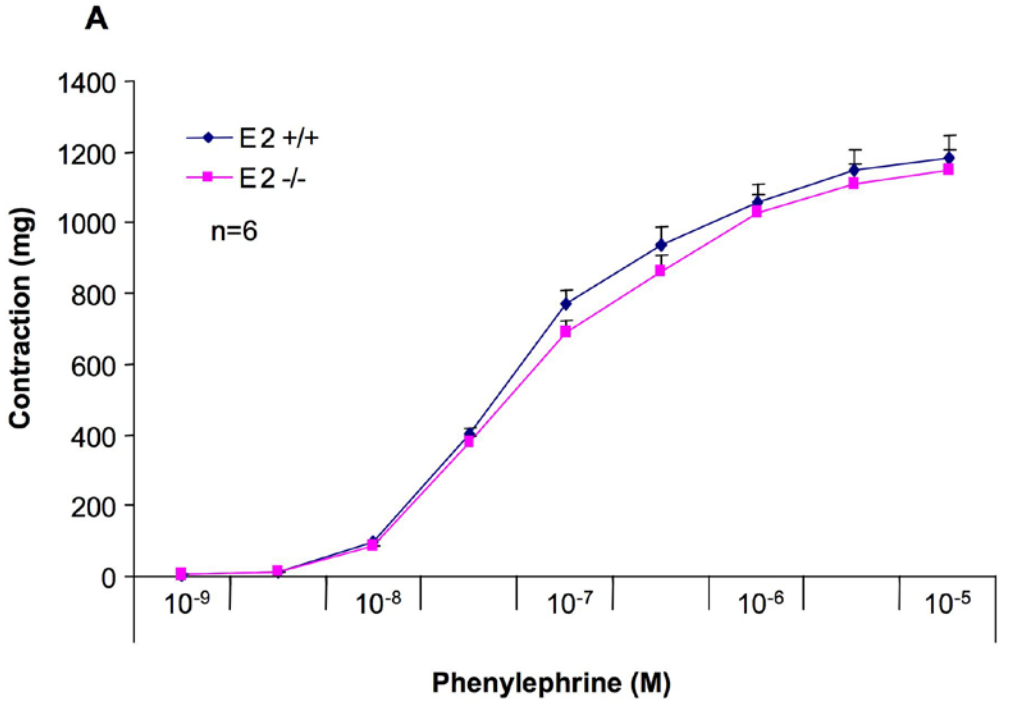
A
1400
1200
1000
800
600
400
200
0
Contraction (mg)
E2 +/+
E2 -/-
n=6
10-9
10-8
10-7
10-6
10-5
Phenylephrine (M)

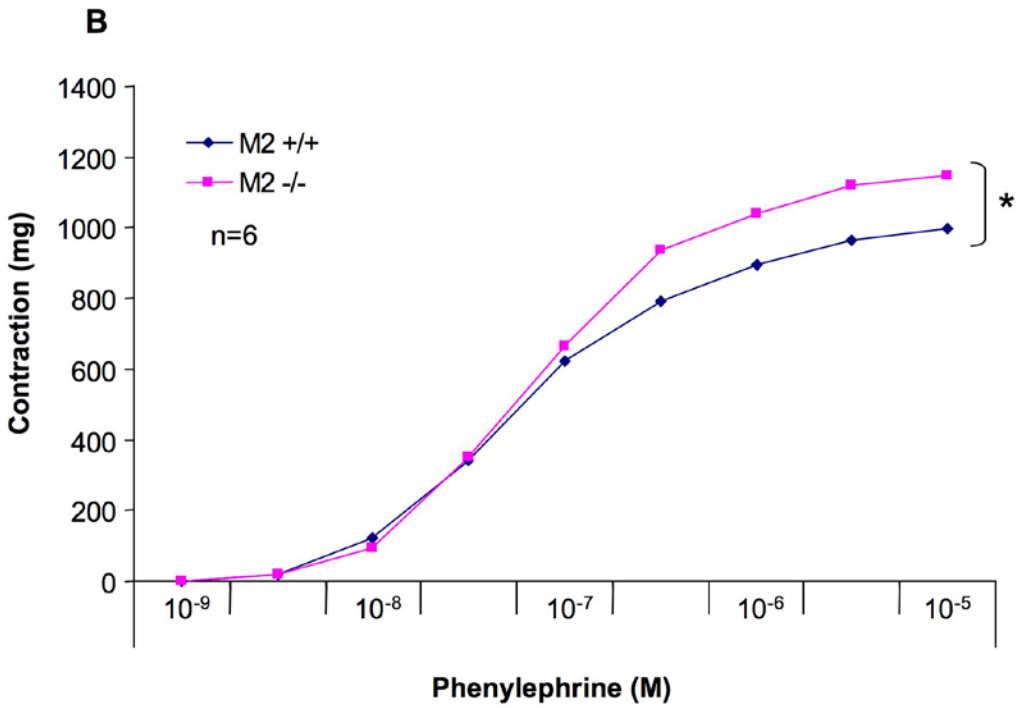
B
1400
1200
1000
800
600
400
200
0
Contraction (mg)
M2 +/+
M2 -/-
n=6
*
10-9
10-8
10-7
10-6
10-5
Phenylephrine (M)

Figure 12: Emilins inhibits TGF-β1 signalling through their EMI-domains.

The CAGA12-lux reporter (500 ng/9.5 cm^2 well) was cotransfected in HEK293T cells with proTGF-$\beta1^{C223S/C225S}$ expression plasmids (300 ng) alone or in combination with Emilin expression plasmids (800 ng) as indicated.

Cells cotransfected with Elastin were used as negative control. Luciferase activity is expressed as percentage of positive control (green bar, no Emilins transfected). TGF-β1 signalling was inhibited by full-length Emilins (blue bars) and EMI domains alone (purple bars), while deletion of EMI domain (red bars) abrogated this activity. Values indicate mean ± SD. (* $p<0,01$).

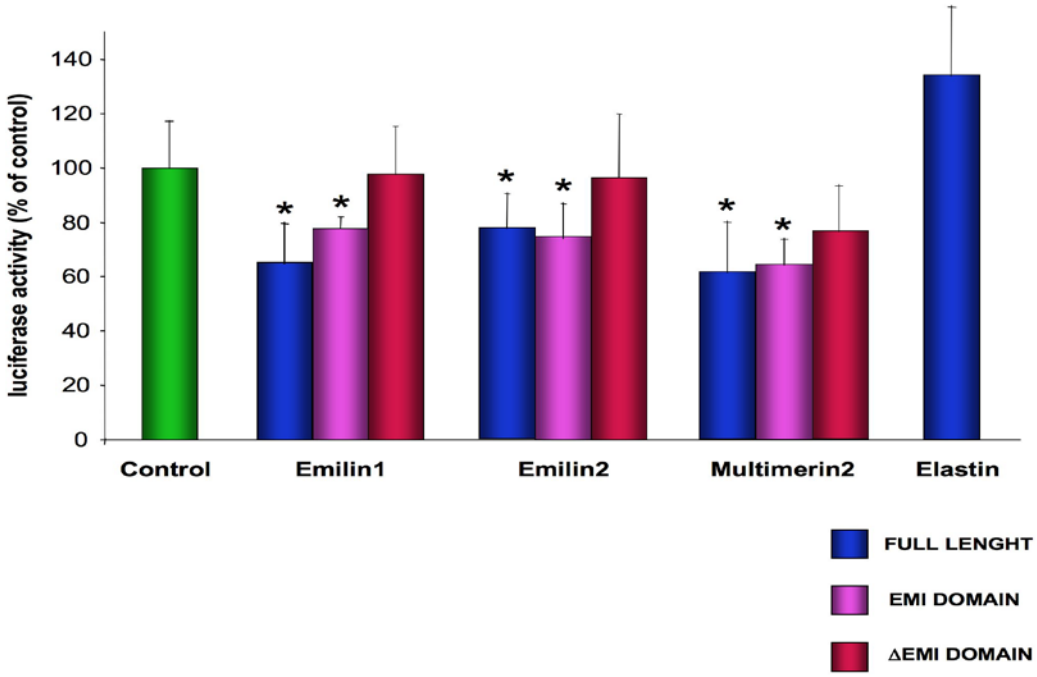
luciferase activity (% of control)
140
120
100
80
60
40
20
0
*
*
*
*
*
*
Control
Emilin1
Emilin2
Multimerin2
Elastin
FULL LENGHT
EMI DOMAIN
ΔEMI DOMAIN

Figure 13: Emilin-2 and Multimerin-2 inhibit proTGF-β1 processing.

HEK293T cells were transfected with proTGF-β1 expression plasmids (0.5 μg/60 mm diameter Petri dishes) and Emilins (12 μg). Western blot of the cell lysates shows that transfected proTGF-β1 is cleaved into LAP and mature TGF-β1 by endogenous convertases (lane 1 and 3). The cleavage is inhibited in the presence of full-length Emilin-1 (lane 2 and 4), Emilin-2 (lane 3) and Multimerin-2 (lane 6).

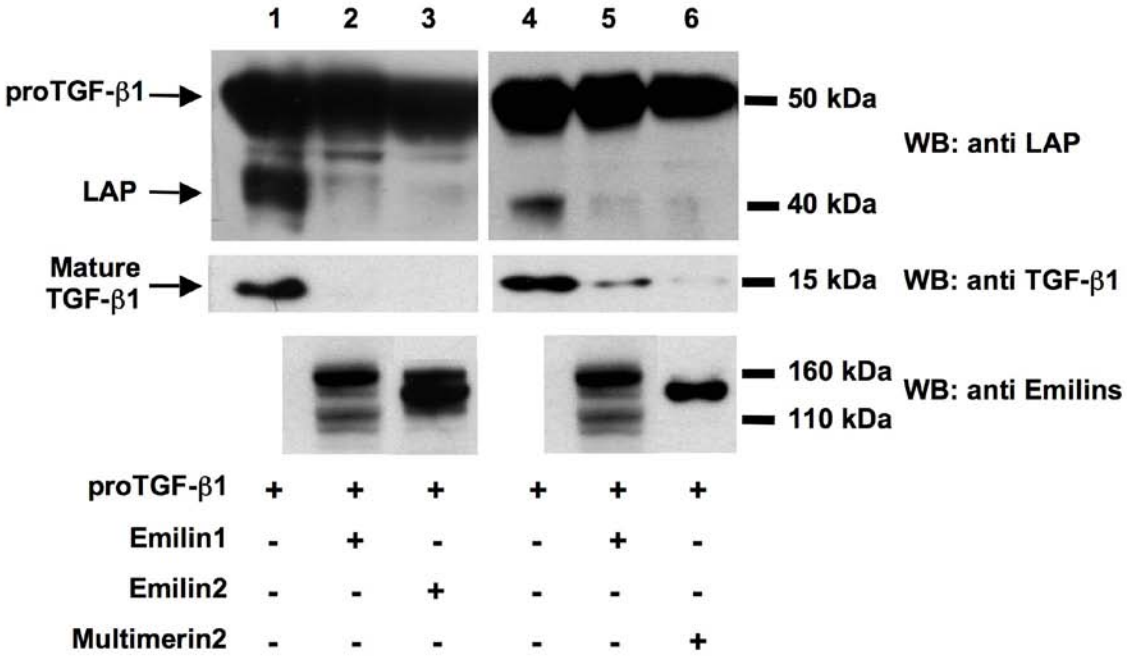
1 2 3 4 5 6
proTGF-β1
LAP
Mature TGF-β1
50 kDa
40 kDa
15 kDa
160 kDa
110 kDa
WB: anti LAP
WB: anti TGF-β1
WB: anti Emilins
proTGF-β1 + + + + + +
Emilin1 - + - - + -
Emilin2 - - + - - -
Multimerin2 - - - - - +

Figure 14: Emilin-2 and Multimerin-2 form a complex with proTGF-β1.

HEK293T cells were transfected with proTGF-β1 (3.5 μg/60 mm diameter dish) and Flag-tagged Emilin2 or Multimerin2 EMI domain-GPI expression plasmids (10.5 μg). Cell lysates were subjected to immunoprecipitation (anti-LAP) and Western blot (anti-FLAG). Both Emilin2 (**A**) and Multimerin2 (**B**) EMI domain coimmunoprecipitated with proTGF-β1.

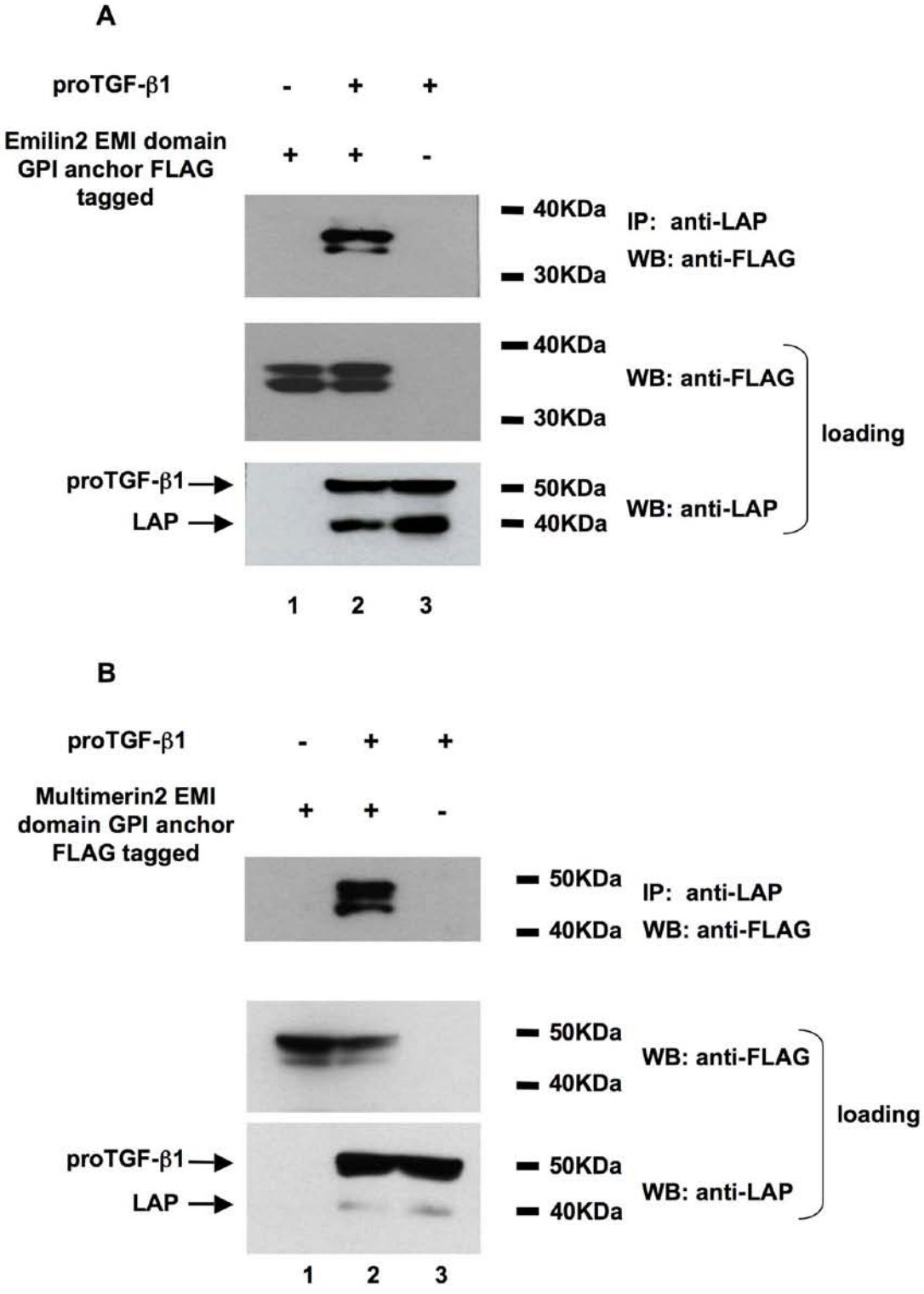
A
proTGF-β1
- + +
Emilin2 EMI domain GPI anchor FLAG tagged
+ + -
40KDa
30KDa
IP: anti-LAP
WB: anti-FLAG
40KDa
30KDa
WB: anti-FLAG
loading
proTGF-β1
LAP
50KDa
40KDa
WB: anti-LAP
1 2 3
B
proTGF-β1
- + +
Multimerin2 EMI domain GPI anchor FLAG tagged
+ + -
50KDa
40KDa
IP: anti-LAP
WB: anti-FLAG
50KDa
40KDa
WB: anti-FLAG
loading
proTGF-β1
LAP
50KDa
40KDa
WB: anti-LAP
1 2 3

Figure 15: Effect of TGF-β1 gene dosage on the hypertensive phenotype of *Mmrn2* and *Emilin2* knockout mice.

Animals with the indicated genotypes were generated by crossing *Emilin* and TGF-β1 double heterozygous animals. Systolic blood pressure was evaluated by tail-cuff plethysmography in conscious mice.

A: reduction of TGF-β1 gene dosage in *Mmrn2* null mice rescued the hypertensive phenotype of these animals.

B: inactivation of a single TGF-β1 allele did not restore systolic blood pressure of *Emilin2* knockout mice to wild type level.

(n = 3 for each genotype). Data are mean ± SEM. *$p < 0.05$ versus wild type mice.

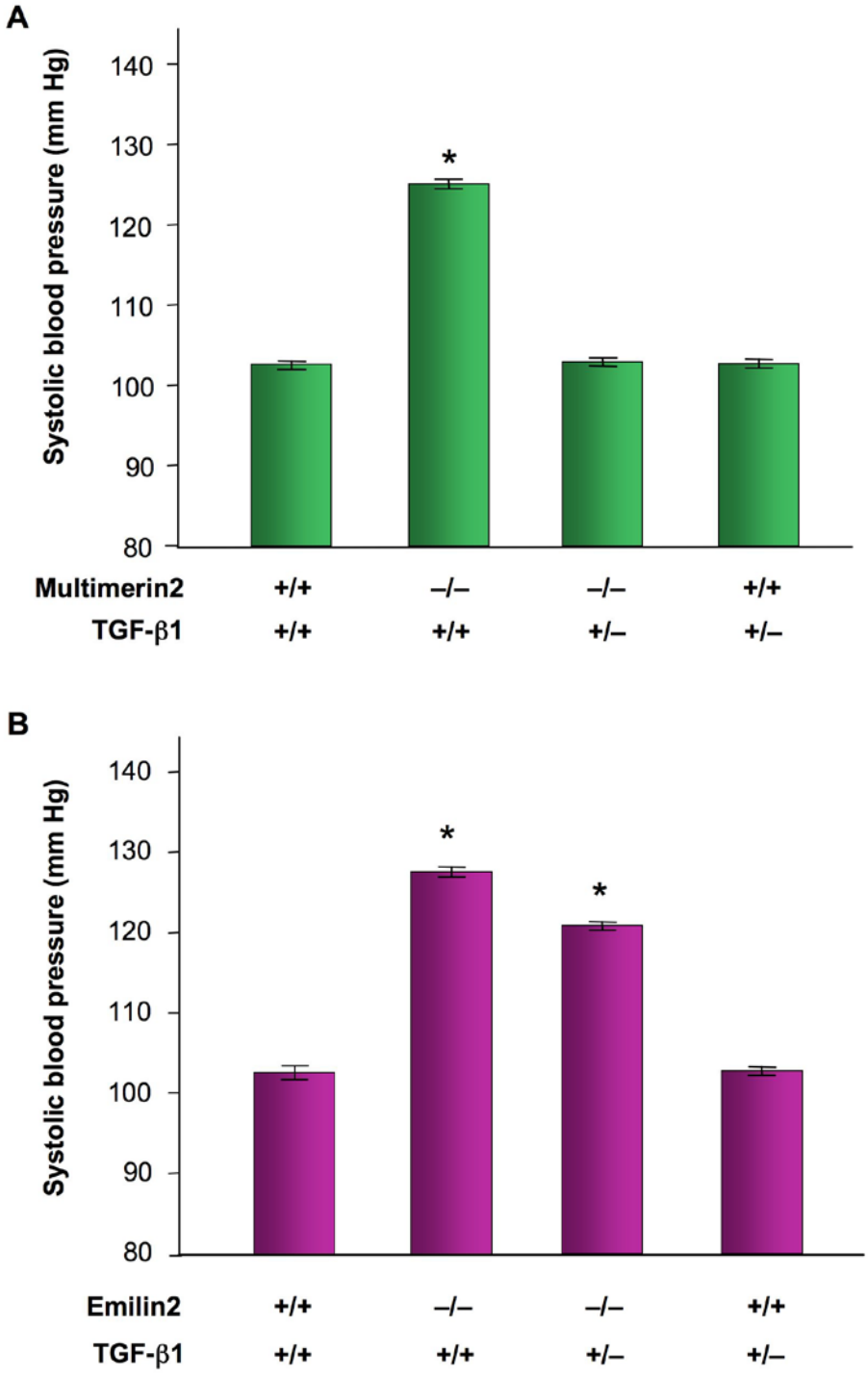
A
Systolic blood pressure (mm Hg)
140
130
120
110
100
90
80
*
Multimerin2 +/+ –/– –/– +/+
TGF-β1 +/+ +/+ +/– +/–
B
Systolic blood pressure (mm Hg)
140
130
120
110
100
90
80
*
*
Emilin2 +/+ –/– –/– +/+
TGF-β1 +/+ +/+ +/– +/–

Figure 16: Emilin-2 reduces proTGF-β2$^{C226S/C228S/C229S}$ and proTGF-β3$^{C228S/C230S}$ activity.

In order to analyse the biological activity of mutant proTGF-β2$^{C226S/C228S/C229S}$ and proTGF-β3$^{C228S/C230S}$, HEK293T cells were transfected with reporter CAGA12-lux in the presence of increasing amount (from 0 to 400 ng/2 cm^2 well) of proTGF-β2$^{C226S/C228S/C229S}$ (**A**) and proTGF-β3$^{C228S/C230S}$ (**B**). Both mutant proTGF-βs were able to induce reporter activity constitutively. HEK293T cells were transfected with CAGA12-lux reporter and proTGF-β2$^{C226S/C228S/C229S}$ (1 μg/9.5 cm^2 well) (**C**) or proTGF-β3$^{C228S/C230S}$ (250 ng/9.5 cm^2 well) (**D**) in combination with Emilin-2 (600 ng/9.5 cm^2 well). Emilin-2 reduced reporter induction in both cases. Luciferase activity is expressed as percentage of positive control (no Emilin-2 transfected). Data are mean ± SD. *$p < 0.01$.

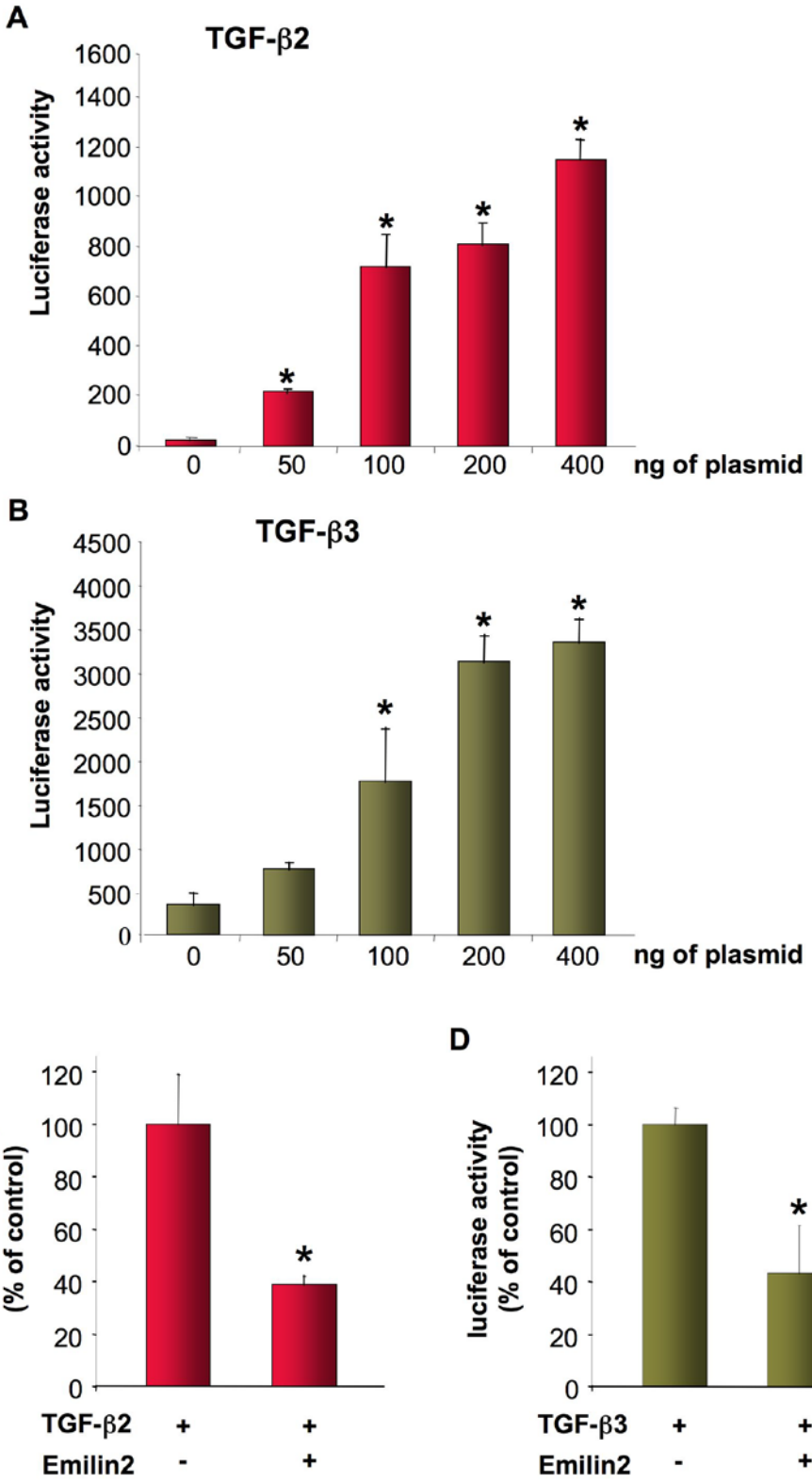
A
TGF-β2
Luciferase activity
1600
1400
1200
1000
800
600
400
200
0
0
50
100
200
400
ng of plasmid
B
TGF-β3
Luciferase activity
4500
4000
3500
3000
2500
2000
1500
1000
500
0
0
50
100
200
400
ng of plasmid
C
luciferase activity (% of control)
120
100
80
60
40
20
0
TGF-β2 + +
Emilin2 - +
D
luciferase activity (% of control)
120
100
80
60
40
20
0
TGF-β3 + +
Emilin2 - +

Figure 17: The hypertensive phenotype of *Emilin2* knockout mice is not rescued by inactivation of a single *TGF-β2* allele.

Systolic blood pressure of mice with a reduction of *TGF-β2* gene dosage in *Emilin2* null background remains higher than the values detected in wild-type animals. Systolic blood pressure evaluated non-invasively by tail-cuff plethysmography in conscious mice. Mice with the indicated genotypes were generated by crossing *Emilin2* and *TGF-β2* double heterozygous animals. Data are mean ± SEM. (n = 3 for each genotype).

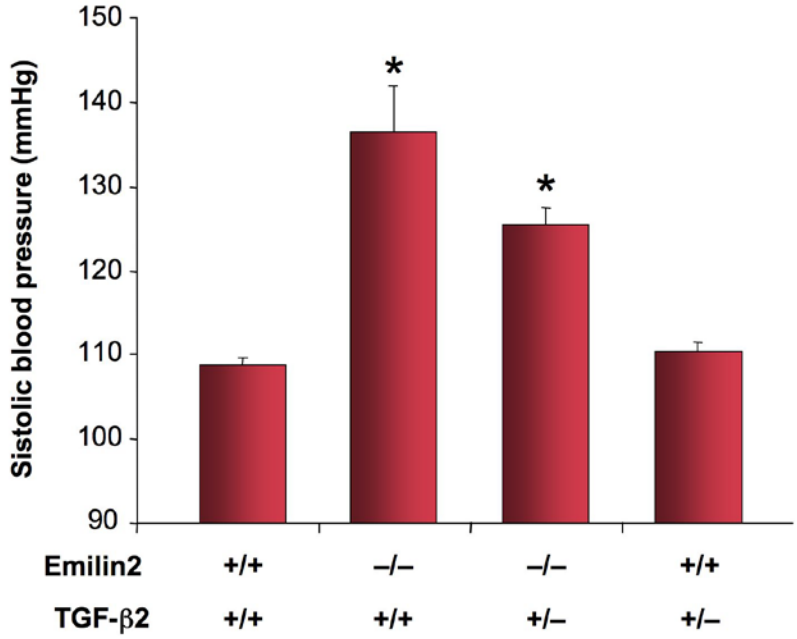
Sistolic blood pressure (mmHg)
150
140
130
120
110
100
90
*
*
Emilin2 +/+ –/– –/– +/+
TGF-β2 +/+ +/+ +/– +/–

Figure 18: Model of Multimerin-2 activity as antagonist of TGF-β1 signalling in the vascular wall.

EC regulates vascular SMC contractility and proliferation through the paracrine effect of TGF-β1. Multimerin-2, by the inhibition of the processing of proTGF-β1, control the availability of this cytokine. Lack of Multimerin-2 increases TGF-β1 signalling and results in an enhanced contractility of vascular SMC to symphatic stimuli and an inhibitions of the proliferation. The increased contraction of the reduction of size of arterial vessels bring to hypertension. An effect on the EC itself remain to be elucidated.

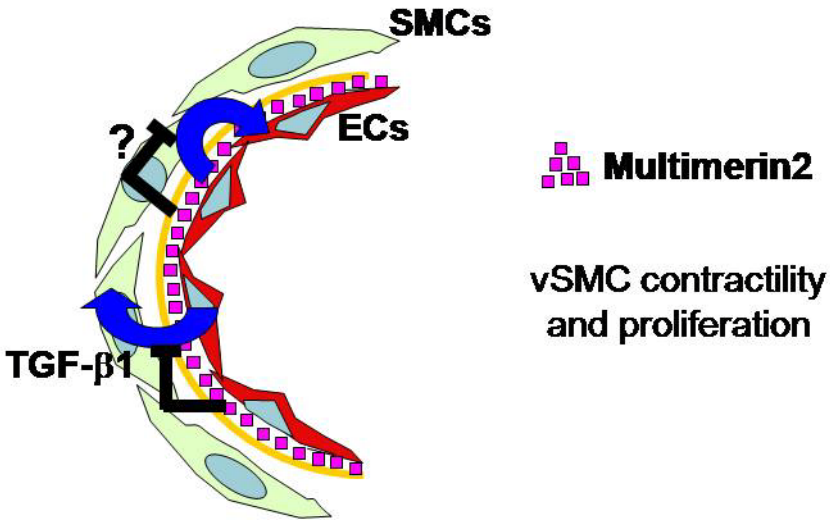
SMCs
ECs
?
TGF-β1
Multimerin2
vSMC contractility
and proliferation